3.2 Combustion Inorganic Transformation

COMBUSTION INORGANIC TRANSFORMATIONS

Sixteenth Quarterly Technical Progress Report
for the Period January through March 1990

by

Chris J. Zygarlicke, Steven A. Benson, Donald L. Toman,
Edward N. Steadman, and David W. Brekke
Combustion and Environmental Systems Research Institute
Energy and Environmental Research Center
University of North Dakota
Box 8213, University Station
Grand Forks, ND 58202

Contracting Officer's Technical Representative: Philip M. Goldberg

for

U.S. Department of Energy
Office of Fossil Energy
Pennsylvania Energy Technology Center

May 1990

Work Performed Under Cooperative Agreement No. DE-FC21-86MC10637

TABLE OF CONTENTS

2 OF 4

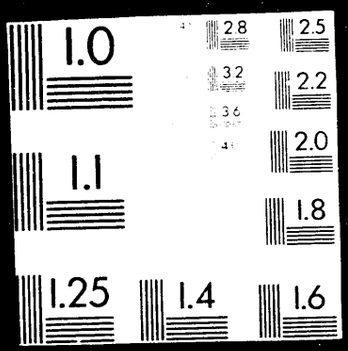

LIST OF FIGURES

LIST OF FIGURES (CONTINUED)

LIST OF TABLES

COMBUSTION INORGANIC TRANSFORMATIONS

EXECUTIVE SUMMARY

Task 1: Improvements to the CCSEM Methodology

Coal samples were prepared for computer-controlled scanning electron microscopy (CCSEM) testing and repeatability testing was begun. Preliminary results of CCSEM precision testing using Beulah coal are reported. The precision of the CCSEM technique is not nearly at the level we desire. Comparison of EERC and PSI CCSEM results for Beulah coal show some discrepancies, especially with the clay minerals and total mineral content. Based on the data it appears we need to analyze more larger-sized minerals in a typical CCSEM run to improve counting statistics.

Discussions with several other groups performing similar analyses were held in preparation for the eventual round robin of the coal standards. Arrangements were made for the purchase and installation of a new automated digital electron microscope/microprobe system (ADEM). The ADEM will provide us with increased automation, new capabilities, and help to alleviate the present sample backlog. The CCSEM image analysis interface was completed, allowing for simultaneous digital image collection during CCSEM analysis.

Task 2: Mineral and Ash Characterization

Fourteen deposits were analyzed for Physical Sciences Incorporated Technology Company (PSIT) for phase assemblage determinations using scanning electron microscopy point-count (SEMPC). The deposits were generated from the following coals: San Miguel, Beulah, Kentucky #11, Illinois #6, Kentucky #9, Eagle Butte, and Upper Freeport.

Task 3: Laboratory-Scale Combustion Testing

Combustion testing of Kentucky #9 and San Miguel coals in the drop-tube furnace was nearly completed. Fly ash was generated at three temperatures for three different size fractions of both coals and collected using both the multicyclone and the impactor. Bulk fly ash samples were also collected on a filter for the unsized and 53-74μm coal feeds. Short residence time chars were generated for the Kentucky #9. All of the samples were submitted for analysis, using either CCSEM or SEMPC.

Particle-size distributions of discrete mineral or amorphous phases in intermediates produced in the drop-tube furnace (DTF) for two coals were examined. Time resolved particle-size distributions (PSDs) of phases show that Beulah and Upper Freeport phases coalesce with time. The Upper Freeport shows an initial increase in the amounts of particles in the lower-size ranges due to fragmentation of minerals or the formation of smaller inorganic ash droplets from submicron minerals or inorganics. The transformation of selected inorganic components through time was also noted. Sodium and calcium organically associated in the Beulah react readily with smaller-sized kaolinitic clays and to a much lesser degree with quartz. Pyrite appears to

undergo fragmentation during combustion in the Beulah and Upper Freeport with a resulting increase in iron oxide.

1.0 GOALS AND OBJECTIVES

The overall objective of this project is the development of a unified picture of the physical and chemical changes that occur in coal inorganic matter during combustion. The research focuses on three main tasks. The first task will involve developing the computer-controlled scanning electron methodology to determine the distribution of mineral grains in pulverized coals. The second task will involve determining the inorganic components in coal and coal ash-derived components for coals and ashes generated in the PETC mineral matter programs at EERC and Physical Sciences, Inc., Technology Company (PSIT). The third task will study the physical and chemical changes of inorganic phases during combustion in laboratory-scale combustion equipment.

The ultimate goal of the project is to develop a means to predict the state (vapor, liquid, or solid), composition, and size of the inorganic material at any point in a combustion system, given the coal composition and combustion conditions. The first task focuses on developing a method to effectively determine the size, composition, and juxtaposition of mineral grains in pulverized coals. In addition, chemical fractionation is used to determine the abundance of organically associated inorganic constituents in the lower rank subbituminous and bituminous coals. Proper determination of the inorganic components in coal is an essential requirement in understanding and ultimately predicting the transformations of inorganic components during coal combustion. The second task involves characterizing coals, chars, and ashes. Coals will be examined by CCSEM and chemical fractionation to determine the association, size, composition, and juxtaposition of the inorganic components in coals.

Chars and ashes produced in Task 3 will be examined to determine their bulk composition, surface composition, phase distribution, and morphology. This will be accomplished primarily by utilizing surface science equipment, scanning electron microscopy/electron microprobe analysis, x-ray fluorescence, and x-ray diffraction. The objective of this task is to follow the transformation of inorganic constituents at various degrees of coal particle burnout to produce the fly ash. The third task involves using the drop-tube furnace system to produce chars at various degrees of burnout and ultimately a carbon-free fly ash. In addition, precisely formulated model mineral/coal mixtures are being produced and combusted to examine in detail some of the transformations that occur. In conjunction with these three tasks is an ongoing effort to evaluate all data produced, with respect to reproducibility, including coal characterization data, char and fly ash formation studies with the drop-tube furnace, and ash characterization data. A means of predicting the fate of inorganic constituents during combustion cannot be adequately developed without consistent, quantitative data. During the past three years, this project has focused on developing consistent and quantitative techniques to produce and analyze the inorganic components in coals, chars, and fly ash. Data is currently available on five coals, and two more will be examined this year. A modeling effort will be initiated this year to predict the size and

composition of ash particles based on coal composition and combustion conditions. This effort will be coordinated with the work presently being conducted at EERC on viscosity modeling (1) and thermochemical equilibrium modeling (2).

Task 1: Improvements to the CCSEM Methodology

The specific objectives of the CCSEM improvements task during this quarter were to:

1) Evaluate the precision of the CCSEM technique using coal samples.

2) Make arrangements for a limited round robin of tested coal samples with other labs.

3) Complete interface of CCSEM computer with image analysis computer to allow for digital image collection.

Task 2: Mineral and Ash Characterization

The specific objective of the mineral and ash characterization task during this quarter was to characterize fourteen deposits for PSIT using SEMPC.

Task 3: Laboratory-Scale Combustion Testing

The specific objectives of the laboratory-scale combustion testing task during this quarter were to:

1) Produce intermediates for Kentucky #9 and San Miguel coal in the drop-tube furnace by combusting three size fractions at 1300, 1400, and 1500°C.

2) Produce intermediates for Kentucky #9 and San Miguel bulk coal samples in the drop-tube furnace and collect on a bulk filter.

3) Produce short residence time chars for the Kentucky #9 coal in the drop-tube furnace at 1500°C for the 53-74 μm coal fraction.

4) Analyze the evolution of fly ash particle-size and composition using CCSEM data of time-resolved intermediates of various test coals.

2.0 TASK 1: IMPROVEMENTS TO THE CCSEM METHODOLOGY

2.1 Introduction

The objective of Task 1 is to provide precise characterization of the mineral matter in coals. Current methods of coal minerals characterization do not provide the level of detail needed to predict the interactions that take place during combustion. Mineral characteristics that affect mineral behavior during combustion include: 1) chemical composition, 2) size, 3) association of minerals with coal matrix, 4) mineralogical associations, and 5) mineral

shape. Presently, coal minerals are being characterized using a computer-controlled scanning electron microscopy/microprobe method (CCSEM). CCSEM analysis gives mineral compositions and sizes. Task 1 seeks to enhance the present methodology to include other significant mineral characteristics, such as the mineral associations, mineral shapes or morphology, and the relationships of the minerals to the coal matrix.

The task 1 project plan will use CCSEM together with an automated image acquisition and characterization program (AIA) to provide the data needed. Initial efforts are focused on testing the accuracy and precision of the present CCSEM methodology and on installing and developing the image analysis system.

2.2 Description of System

The SEM/microprobe system at the EERC consists of a JEOL 35U scanning electron microscope/microprobe, a GW electronics backscatter electron detector, an ultrathin window energy-dispersive x-ray detector, a wavelength dispersive x-ray detector, digital beam control, a Tracor-Northern 5600 x-ray microanalyzer control system, a Tracor-Northern 8500 image analyzer, and stage automation. The Tracor-Northern 5600 is interfaced with a MicroVax II and personal computer system for advanced data manipulation.

The key components of the SEM system that make it possible to image, size, and analyze inorganic particles include the backscatter electron detector, digital beam control, and the ultrathin window energy dispersive x-ray detector. The Tracor-Northern 5600 image analysis system allows for the automated acquisition and beam control, with data storage accomplished using the MicroVax II or a PC. The Tracor-Northern 8500 image analysis system allows for the automated acquisition, storage, and processing of images from the SEM. Figure 1 shows a schematic of the system hardware including the newly acquired image analysis components installed during this reporting period.

The CCSEM analysis uses backscattered electron imaging (BEI) and energy-dispersive spectra (EDS) detection to analyze minerals. Since the mineral or ash particles appear brighter in BEI relative to the lower atomic number background of the matrix, a distinction can be made between coal, epoxy, and mineral grains. Using the Tracor-Northern particle recognition and characterization program, the electron beam is programmed to scan over the field of view to locate the bright inclusions that correspond to mineral or ash species. On finding a bright inclusion, the beam performs eight diameter measurements on the inclusion, finds the center of the inclusion, and collects an EDS for two seconds. The system is set up to analyze 12 elements: Na, Mg, Al, Si, P, S, Cl, K, Ca, Fe, Ba, and Ti. The associated computer system then outputs to a storage file the following information for each particle analyzed: the size, area, perimeter, chemical composition, coordinates of location on the sample surface, frame number, and number of energy-photon counts.

Data from the CCSEM analysis is transferred simultaneously to a personal computer or the MicroVax II, where it is stored on tape or disk. Software developed at EERC classifies the minerals into categories based on size and composition.

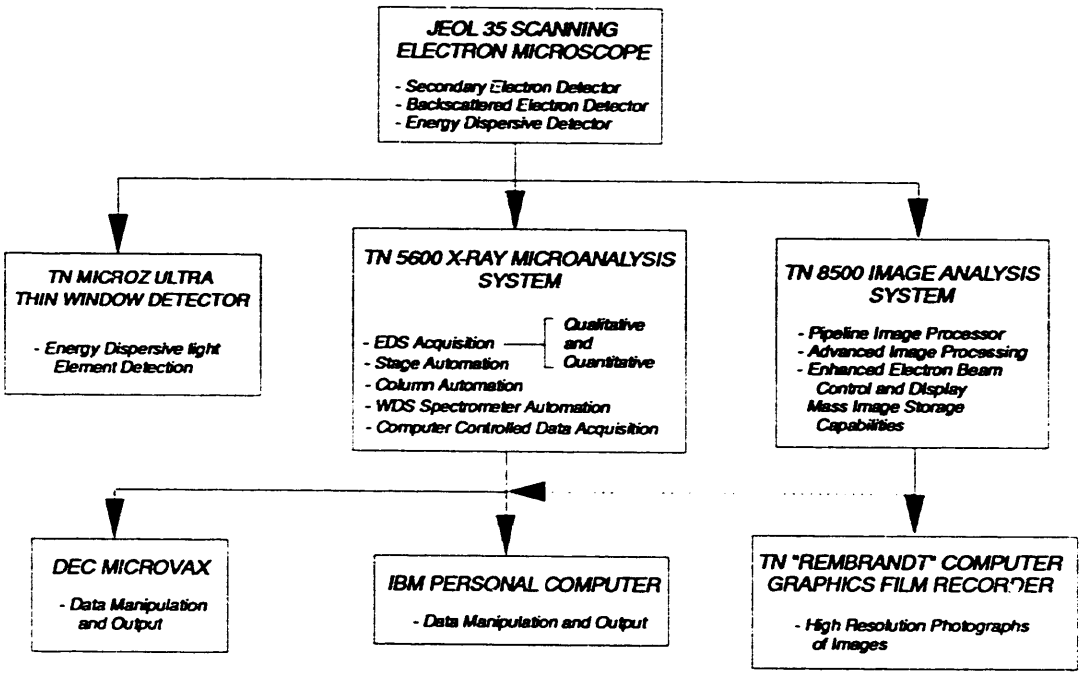

Figure 1. Schematic of SEM/microprobe system and its operation.

2.3 Subtask A: CCSEM Testing

Three coals were chosen for CCSEM precision testing and eventual round robin testing with other labs. These coals are: 1) Beulah (lignite), 2) Eagle Butte (subbituminous), and 3) Illinois #6 (bituminous). These coals were chosen from the suite of coals being investigated by both PSI and EERC. These coals are presently being prepared by several techniques to determine the best methods for obtaining reproducible samples.

CCSEM testing on mineral standards reported in previous Quarterly reports showed fairly good precision (3). Results are reported here for precision testing of the size-fractionated Beulah test coal and bulk Beulah coal. EERC results are also compared to those obtained by PSI (4).

Table 1 shows CCSEM results for the Beulah samples. The major mineral categories of kaolinite, pyrite, and quartz are fairly consistent between all 4 analyses. Total mineral contents on a coal basis are not as consistent. The particle-size distributions of the minerals were plotted for all four samples as shown in Figure 2. There is a considerable spread in the size distribution data. More detailed examination of the raw data seems to indicate that most of the differences between samples are the result of a few, relatively large, particles. This preliminary data seems to indicate a need to analyze more particles in the larger size range. Similar work is being performed using Upper Freeport coal and will be reported in the final report.

TABLE 1

PRECISION TESTING RESULTS OF SELECTED BEULAH MINERALS
(Weight Percent)

	Run 1 *	Run 2 *	Run 3 **	PSI **
Quartz	18.00	17.61	16.3	12.0
Aluminosilicate ***	41.72	34.42	42.6	43.0
Ca-aluminosilicate	0.17	0.91	0.5	1.0
Fe-aluminosilicate	0.28	0.90	0.5	--
K-aluminosilicate	0.79	1.24	1.0	1.0
Pyrite	25.6	25.8	24.2	26.0
Gypsum	2.13	2.94	3.1	--
Barite	1.58	0.67	2.0	--
Ca-Rich	0.03	0.00	0.0	1.0
Si-Rich	0.31	0.30	0.7	--
Unknown	6.83	10.47	5.4	10.0
TOTAL Minerals Coal Basis	5.58	3.37	7.3	7.0

* 53-74 µm coal
** Bulk coal
*** PSI mixed silicate and kaolinite contents added to get this amount

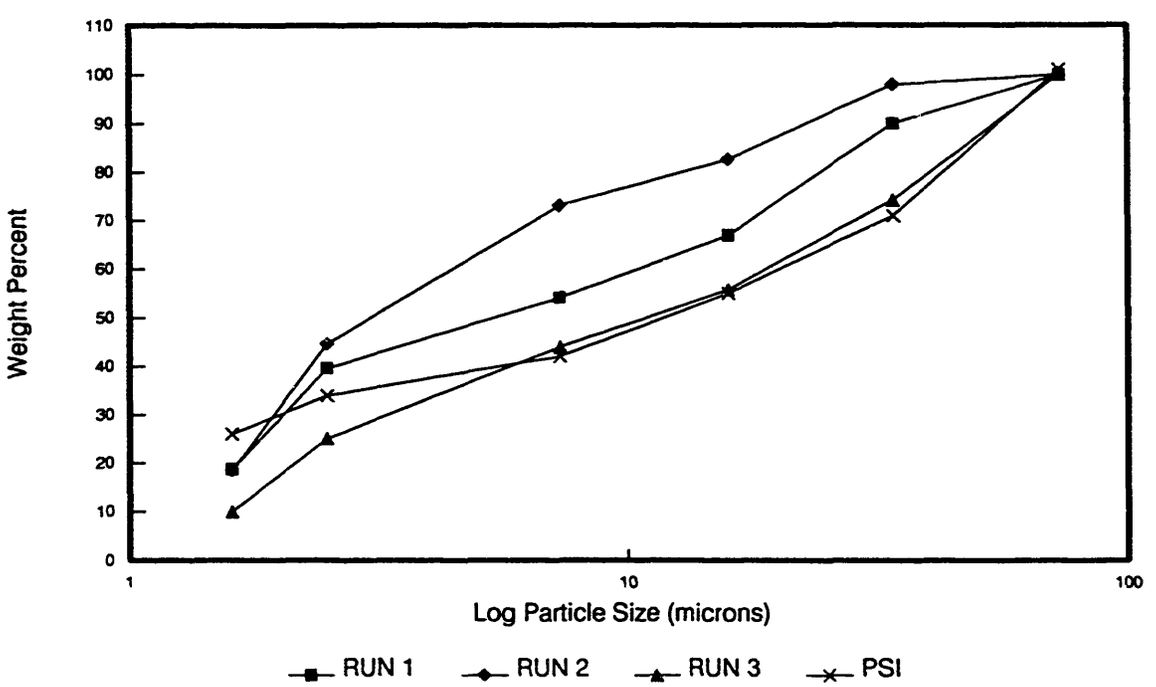

Figure 2. Reproducibility of particle size distributions determined for the samples listed in Table 1.

Discussions were held with Dr. G. P. Huffman of the University of Kentucky and Dr. W. E. Staszheim of Ames Laboratory, Iowa State University, concerning a round robin of one or more of the coals for reproducibility testing. A limited round robin of samples with these labs will be started during the next quarter.

2.4 Subtask B: CCSEM Automation and Development

Work in the area of CCSEM automation and development has focused on the automation of the present analysis and the establishment of an interface, allowing for the transfer of CCSEM field areas to the image analysis system for automated image collection and storage. Work on both of these areas is now complete, and these routines are both being tested. The automated digital image collection program was completed since the last reporting period and is briefly described below. The standard CCSEM analysis is run in the normal manner, but prior to the analysis of each frame examined, a backscattered digital image is obtained and saved to the TN8500 image analysis system. As the CCSEM analysis procedure proceeds, each particle analyzed is identified on the image. The positional data is saved to a disk along with the standard CCSEM data. These data can be recalled at a later time in order to make determinations of mineral associations and the relationships of the mineral particles to the coal matrix (juxtaposition). The data file is then appended to include any juxtapositional data. This program is seen as an intermediate step in development of the new CCSEM program which will provide juxtapositional relationships in an automated fashion.

2.5 Conclusions

Coal standards were selected and work has begun on reproducibility testing for the CCSEM analysis. Provisions are presently underway for a limited round robin of coal samples with G. P. Huffman and W. E. Straszheim. The CCSEM program is now fully automated, and the simultaneous digital image collection is in place as well.

Preliminary results of CCSEM precision testing using Beulah 53-74 μm coal revealed that the technique is not nearly at the precision level we desire. Comparison of EERC and PSI CCSEM results for Beulah and Upper Freeport coals shows some discrepancies, especially with the clay minerals and total mineral content. Based on the data, it appears we need to analyze more larger-sized minerals in a typical CCSEM run to improve counting statistics.

3.0 TASK 2: MINERAL AND ASH CHARACTERIZATION

3.1 Introduction

The important thrust of this task is to determine the inorganic constituents of coal, char, and fly ash using computer-controlled scanning electron microscopy (CCSEM), scanning electron microscopy point count (SEMPC), Auger electron spectroscopy (AES) and x-ray photoelectron spectroscopy (XPS). Samples will be generated from drop-tube furnace reactors at both the Energy and Environmental Research Center (EERC) and Physical Sciences Incorporated

(PSIT). Also included in this task is a separate 3-year study of inorganic transformations observed for the Robinson and Eagle Butte coals combusted in a down-fired combustor.

3.2 Equipment and Procedures

Computer-controlled scanning electron microscopy (CCSEM) utilizes a computer program to locate, size, and analyze particles. Because the analysis is automated, a large number of particles can be analyzed quickly and consistently. The main component of the CCSEM analysis systems is the annular backscattered electron detector (BES). The BES system is used because the coefficient of backscatter (the fraction of the incoming beam that is backscattered) is proportional to the square root of the atomic number of the scattering atoms. This permits a high degree of resolution between sample components based on their atomic numbers. This means that minerals can be easily discerned from the coal or char matrix, and fly ash particles can be easily discerned from epoxy in polished sections. Brightness and contrast controls are used to optimize threshold levels between the coal or char matrix and mineral grains or fly ash particles. When a video signal falls between these threshold values, a particle is discerned, and the particle center is located. A set of eight diameters about the center of the particle is measured, and the particle area, perimeter, and shape are calculated. The beam is then repositioned to the center of the particle, and an x-ray spectrum is obtained. The information is then stored for data reduction and manipulation. The CCSEM data provides quantitative information concerning the discrete mineral species or noncrystalline inorganic phases present and their size and shape characteristics. Since the same analysis can be performed on the initial coal, char, and resultant fly ash, direct comparisons can be made and inorganic transformations inferred.

In addition to the CCSEM analysis of coals to determine size and type of minerals, the technique has recently been expanded to determine the juxtaposition of minerals; i.e., how minerals are associated with each other and whether mineral grains are associated within coal particles (inherent) or associated extraneously to coal particles. This information is extremely important with respect to understanding the transformations of inorganic constituents during combustion. In order to perform such an analysis, image analysis is employed that allows for detailed examination and manipulation of stored SEI and BEI images and x-ray maps. Inherent and extraneous minerals and associations of adjacent minerals are determined easily by examining stored images of coal-epoxy polished surfaces. This technique is currently under development at the EERC.

Characterization of fly ash was performed using scanning electron microscopy and electron microscopy analysis. A technique was developed at the Energy and Environmental Research Center to determine the relative abundance of phases present in ashes and deposits (5). The technique is called SEM point count or SEMPC. The method involves microprobe analysis of about 250 random points in a polished cross section of sample. The quantitative analysis of each point is transferred to a computer file for data base analysis. New Fortran software is used to calculate molar and weight ratios for each point. Using these ratios, the points that have compositions of known phases (common to ashes and coal minerals) are identified and counted.

The software then finds the relative number of unknown phases. The unknown phases are those for which there are no known phases corresponding to the chemical composition. For this study, it was assumed that these points were amorphous. In addition, the average chemical composition of all the points in the sample was calculated.

X-ray photoelectron spectroscopy (XPS) and Auger spectroscopy were used to characterize the surface of the fly ash and char. The XPS technique determines the binding energy of an electron removed from the outer 50 angstroms of the surface due to the impingement of beam x-rays. The binding energy of the electrons is a function of the elements present and their electronic environment. Thus XPS can be used to determine both the species present on the surface and their chemical compositions. The auger technique uses the electron beam as the ionization source, and the auger electrons that come from the secondary electron emission are measured. This technique can provide chemical composition data for very small areas on the order of one square micrometer. Thus the auger technique can be used to examine the first 20- to 50-angstrom depths of surface layers of individual fly ash particles.

Another surface analysis technique performed at the EERC is secondary ion mass spectroscopy (SIMS). SIMS is a surface analysis and depth profiling technique that utilizes an ion beam to bombard the sample. This produces emissions of positive and negative secondary ions from the surface. These ions, both individual and clusters of atoms, are mass-analyzed with an energy-filtered quadruple mass spectrometer. The technique is used for trace impurity analysis and offers extremely high detection sensitivity for many elements, full elemental detection (include hydrogen), and the ability to provide isotopic and molecular information.

3.3 Results of SEMPC Analysis of PSIT Deposits

As part of collaborative efforts between EERC and PSIT, fourteen deposits generated by PSIT were analyzed using SEMPC. The deposits, listed in Table 2, were generated from the following coals: San Miguel, Beulah, Kentucky #11, Illinois #6, Kentucky #9, Eagle Butte, and the Upper Freeport. Table 3 summarizes the phase and oxide compositions for the deposits.

4.0 TASK 3: LABORATORY-SCALE COMBUSTION TESTING

4.1 Introduction

Coals contain a complex suite of inorganic species that include significant quantities of both organically associated cations and discrete minerals. Problems associated with inorganic constituents in coal combustion systems include ash deposition, fine particulate formation, and corrosion and erosion of boiler parts. Of specific interest are the interactions between those inorganic constituents that result in the formation of low melting point phases during combustion and gas cooling. These phases are often the cause of ash deposition problems on boiler heat transfer surfaces. The formation of these low melting point phases is a result of a combination of complex

TABLE 2

PSI DEPOSIT SAMPLE LABELS AND EERC SAMPLE NUMBERS

Sample Label
San Miguel SM-3
San Miguel SM-5
San Miguel SM-6
San Miguel SM-11
Beulah Lignite BL-19
Beulah Lignite BL-21
Beulah Lignite BL-29
Kentucky #11 KY-2
Kentucky #11 KY-5
Illinois #6 IL-4
Illinois #6 IL-5
Kentucky #9 KY-16
Eagle Butte EB-17
Upper Freeport UF-13

physical and chemical transformations of inorganic components of coals duringcombustion studied in a drop-tube furnace designed to simulate the time-temperature profile of a pulverized coal-fired utility boiler. The chemical and physical transformations of the inorganic constituents depend upon their association in the coal and upon combustion conditions. Volatilization and condensation of sodium is one of the key transformations that the drop-tube furnace project is investigating to gain insight into the formation of liquid phases in and on the surfaces of entrained ash particles. The primary objectives of the drop-tube furnace task are to determine the factors that affect the size and composition of the fly ash.

4.2 Equipment and Procedures

4.2.1 Drop-Tube Furnace System

The drop-tube furnace is a laboratory-scale, entrained flow tube furnace with the ability to combust coal and produce ash under closely controlled conditions. Combustion parameters such as initial hot zone temperature, residence time, and gas cooling rate can be closely controlled and monitored.

The furnace system is housed in a three-floor laboratory specifically designed for clean and efficient operation of the system, as shown in Figure 3. The furnaces are mounted on furnace bars extending through all three levels and can be moved to accommodate specific applications. The adjoining control room provides a clean, climate-controlled environment for the electronic equipment associated with the drop-tube system.

TABLE 3

SEMPC ANALYSIS OF PSIT DEPOSITS
(EDS Weight Percents)

Phase Composition	SM-3	SM-5	SM-6	SM-11	BL-19	BL-21	BL-29	KY-2	KY-5	IL-4	IL-5	KY9-16	EB-17	UF-13
Gehlenite	0.0	0.0	0.8	0.0	3.7	15.8	6.0	0.0	1.8	0.0	0.0	0.0	5.5	0.0
Anorthite	1.2	0.6	0.8	1.1	1.9	0.0	0.0	10.3	5.5	1.8	1.7	0.0	3.6	0.0
Pyroxene	0.0	0.0	0.0	0.0	0.0	1.8	0.0	0.0	0.0	0.0	0.0	0.0	1.8	1.8
Mullite	0.0	0.0	0.0	0.0	0.0	0.0	0.0	0.0	0.0	0.0	10.3	0.0	1.8	0.0
Calcium Silicate	0.0	0.0	0.0	0.0	0.0	0.0	2.0	0.0	0.0	0.0	0.0	0.0	0.0	0.0
Quartz	7.8	6.3	47.7	8.9	33.3	0.0	14.0	15.5	29.1	5.5	8.6	26.2	12.7	35.7
Iron Oxide	0.6	0.0	1.2	0.7	18.5	3.5	2.0	19.0	7.3	5.5	8.6	7.1	3.6	7.1
Calcium Oxide	0.0	0.0	0.8	0.0	0.0	1.8	0.0	0.0	0.0	0.0	0.0	0.0	0.0	0.0
Ankerite (Ca,Mg,Fe) CO_3	0.0	0.0	0.4	0.0	0.0	0.0	0.0	0.0	0.0	0.0	0.0	0.0	0.0	0.0
Aluminum Oxide	0.0	0.0	0.0	0.0	0.0	0.0	0.0	0.0	0.0	0.0	1.7	0.0	0.0	0.0
Pure Kaolinite (Amorp.)	0.6	2.5	0.4	0.7	0.0	0.0	0.0	0.0	0.0	0.0	15.5	0.0	1.8	1.8
Kaolinite Derived	0.0	1.3	0.4	0.0	0.0	3.5	0.0	0.0	7.3	25.5	1.7	2.4	5.5	0.0
Illite (Amorp.)	26.9	19.6	9.5	15.1	0.0	5.3	2.0	3.4	5.5	9.1	8.6	7.1	1.8	7.1
Montmorillonite (Amorp.)	0.0	0.0	0.0	0.0	0.0	0.0	0.0	0.0	0.0	0.0	0.0	14.3	0.0	0.0
Calcium Derived	0.0	0.0	0.4	0.0	0.0	0.0	0.0	0.0	0.0	0.0	0.0	0.0	0.0	0.0
Unclassified	62.9	69.6	37.4	73.4	42.6	68.4	74.0	51.7	43.6	52.7	43.1	42.9	61.8	46.4
Oxide Composition														
SiO_2	70.6	70.0	82.6	72.1	51.6	37.5	37.3	49.4	63.4	55.5	44.1	56.6	45.8	65.4
Al_2O_3	17.3	17.8	7.5	15.8	7.8	18.5	7.6	13.7	12.9	20.8	31.7	13.3	17.3	14.2
Fe_2O_3	2.3	1.2	3.0	1.6	23.4	5.2	8.9	24.6	10.9	11.9	16.3	15.0	9.9	12.6
TiO_2	0.9	1.2	0.7	1.2	0.5	0.9	2.1	0.5	1.1	1.0	0.4	1.1	1.0	0.5
P_2O_5	0.0	0.0	0.0	0.0	0.0	0.0	0.0	0.0	0.1	0.0	0.0	0.1	0.2	0.0
CaO	3.6	4.1	3.0	3.9	10.8	21.9	33.8	6.5	6.4	4.7	3.5	6.2	18.6	1.8
MgO	0.5	0.6	0.3	0.5	2.3	6.2	1.3	1.3	0.8	1.5	0.6	0.7	4.1	0.8
Na_2O	1.5	1.7	0.5	1.5	0.9	5.0	0.2	1.0	0.5	0.8	0.6	0.2	0.4	0.4
K_2O	2.7	2.5	1.0	2.2	0.8	2.9	3.6	1.7	2.1	3.0	2.0	3.2	1.3	2.2
SO_3	0.1	0.2	0.3	0.2	0.3	0.6	2.9	0.3	0.2	0.1	0.2	2.1	0.7	0.3
BaO	0.2	0.1	0.1	0.2	0.6	0.9	0.7	0.1	0.1	0.1	0.0	0.1	0.2	0.1
MN_2O_7	0.1	0.2	0.1	0.2	0.4	0.2	0.1	0.2	0.3	0.1	0.1	0.1	0.2	0.4
ClO	0.2	0.3	0.8	0.6	0.6	0.1	1.5	0.8	1.2	0.5	0.5	1.2	0.2	1.3

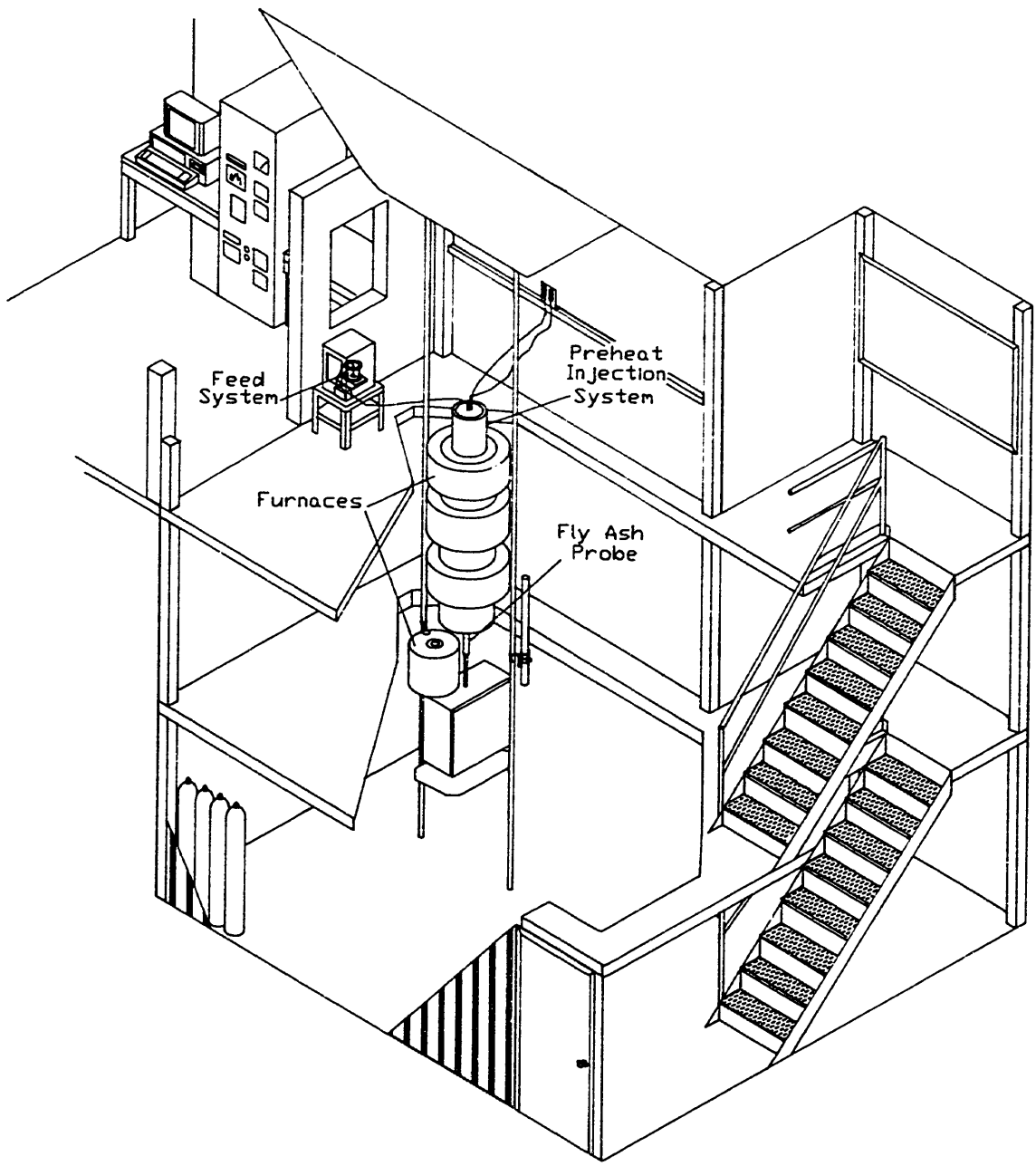

Figure 3. Drop-tube furnace laboratory.

The furnace assembly consists of a series of vertically oriented tube furnaces illustrated in Figure 4. These furnaces possess a total of four independently controlled, electrically heated zones. Each of these furnaces can be used separately or in conjunction with the other furnaces. This allows for maximum flexibility and precise control over combustion conditions.

Coal, primary air, and secondary air are introduced into the furnace system by means of a preheat injector. This system injects ambient-temperature primary air and coal into the furnace from a water-cooled probe assembly at the center of the tube. Secondary air is typically heated to 1000°C and introduced into the furnace through a mullite flow straightener. Thus the material to be combusted is introduced into the top of the furnace, along with preheated secondary air, and travels down the length of the furnace in a laminar flow regime.

The coal feed system is designed to feed particles of various sizes in the pulverized coal range at rates of 0.05 to 0.5 grams per minute and at primary carrier gas rates of approximately one liter per minute. The basic apparatus shown in Figure 5 consists of a pressurized cylinder in which a container filled with coal is placed. A rotating brush and stirrer attached to a variable speed motor feeds the coal from the container into a funnel where it is transported through the feed tubing into the furnace injector by the carrier gas.

Fly ash is cooled by means of a fly ash quenching probe shown in Figure 6. This system is reliable and versatile. Several collection devices can be added to the probe to collect the fly ash.

Size-segregating methods of fly ash collection are being employed. The Environmental Protection Agency Southern Research Institute Five-Stage Cyclone (EPAFSC) is being used on a routine basis to collect fly ash. The EPAFSC is designed to make five equally spaced particle size cuts (D_{50}) on a logarithmic scale within the range of 0.1-10 millimeters. The advantage of this system is its capability of collecting the relatively large sample amounts needed for subsequent chemical and morphological analyses.

In addition to the EPAFSC, the University of Washington Mark 5 Source Test Cascade Impactor (STCI) is used during selected combustion tests. The STCI was developed as a means of measuring the size distribution of particles in stacks and ducts at air pollution emission sources. The Mark 5 impactor produces size cuts of fly ash particles by inertial separation. These data will be used for comparison with the EPAFSC data and to provide more detailed information concerning the effects of combustion conditions on the size distribution of the fly ashes.

A short residence time probe was designed and constructed to collect ash samples at any residence time. The probe consists of a series of four concentric, water-cooled, steel tubes. The outer shell is for introducing the quench gas at the top of the probe. The innermost shell removes the combustion gases, and the remaining shells carry the cooling water. The probe is covered with an alumina-insulating cylinder two inches in outside diameter (Figure 7).

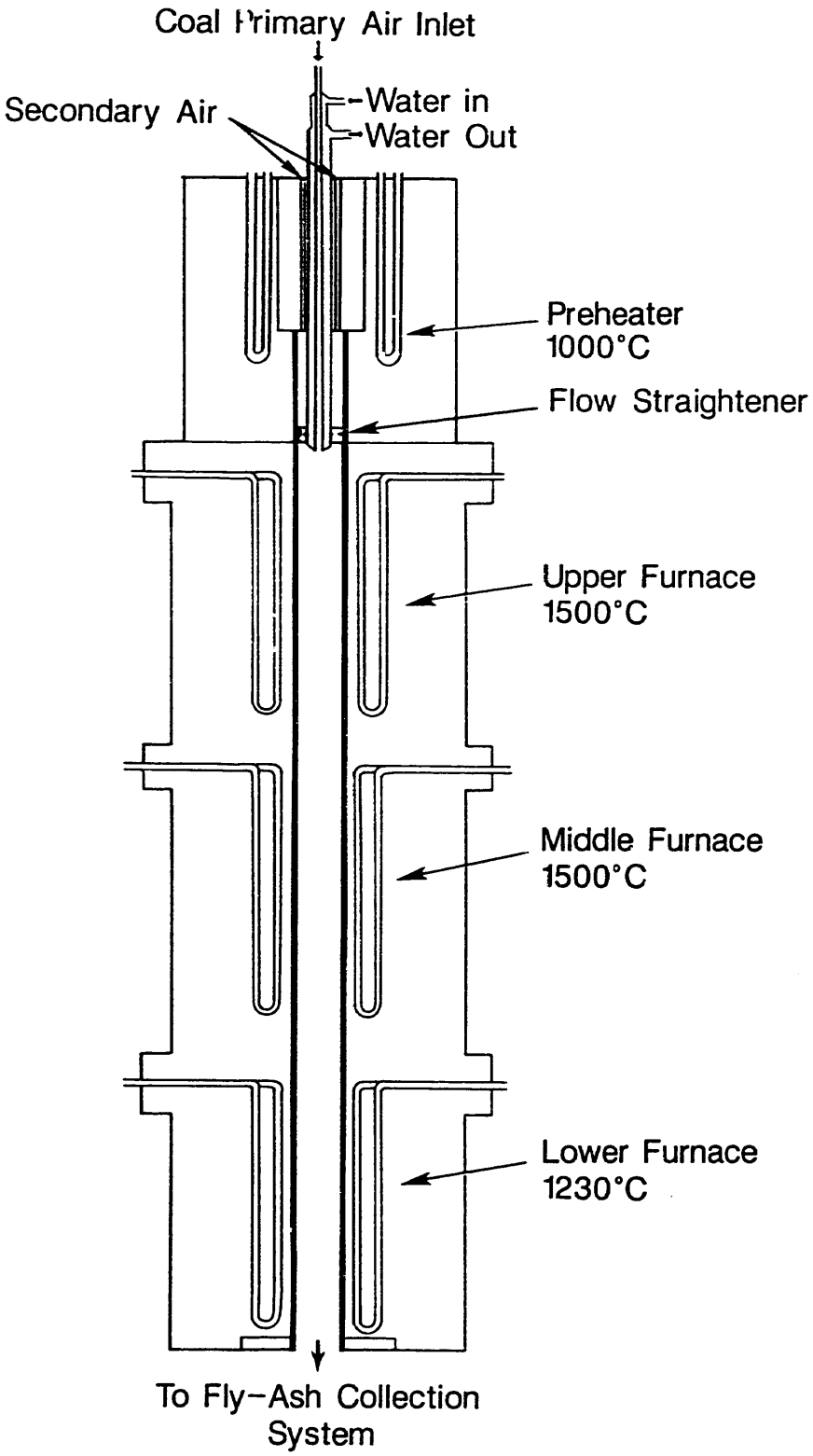

Figure 4. Cross-sectional diagram of the drop-tube furnace.

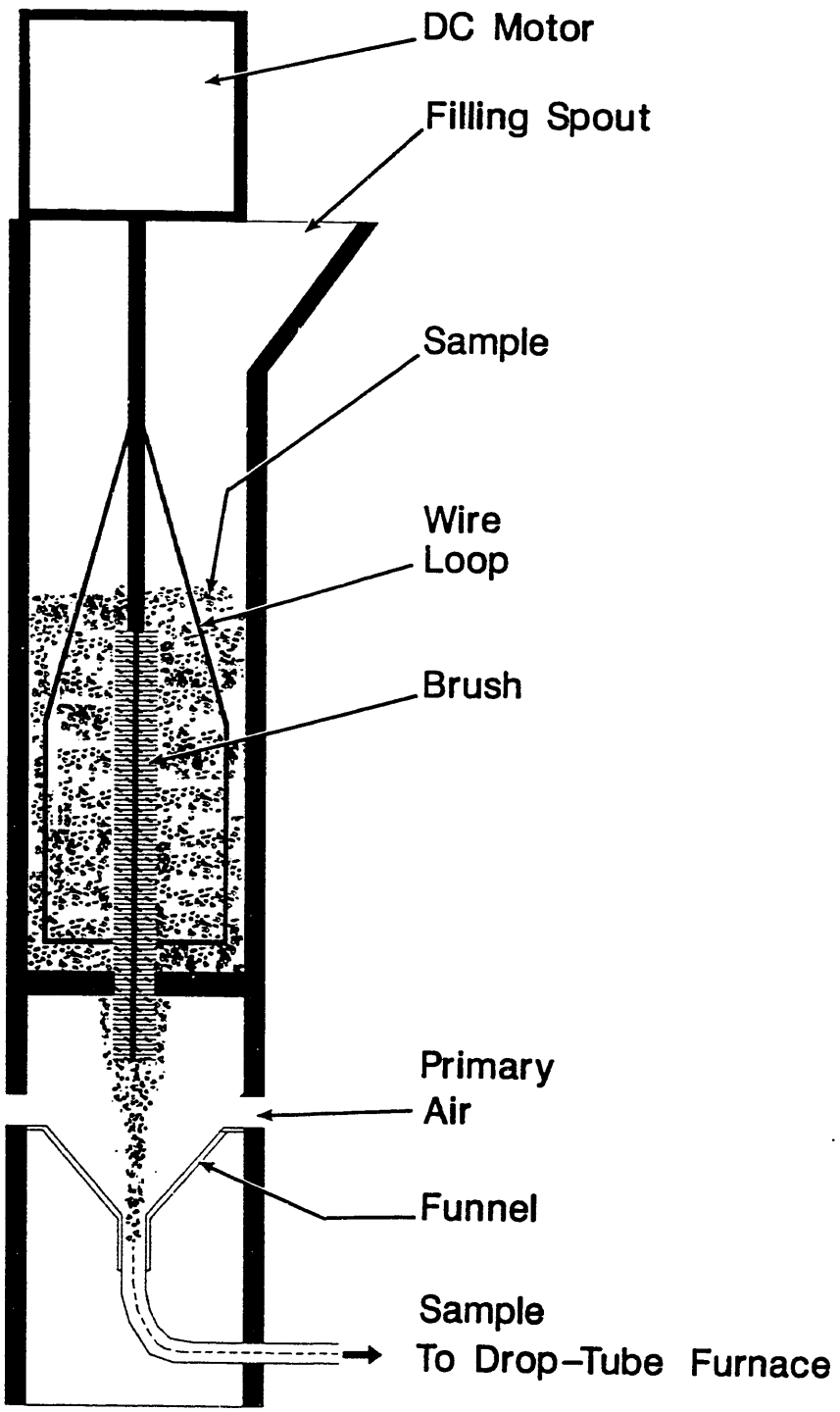

Figure 5. Coal feeder for the drop-tube furnace.

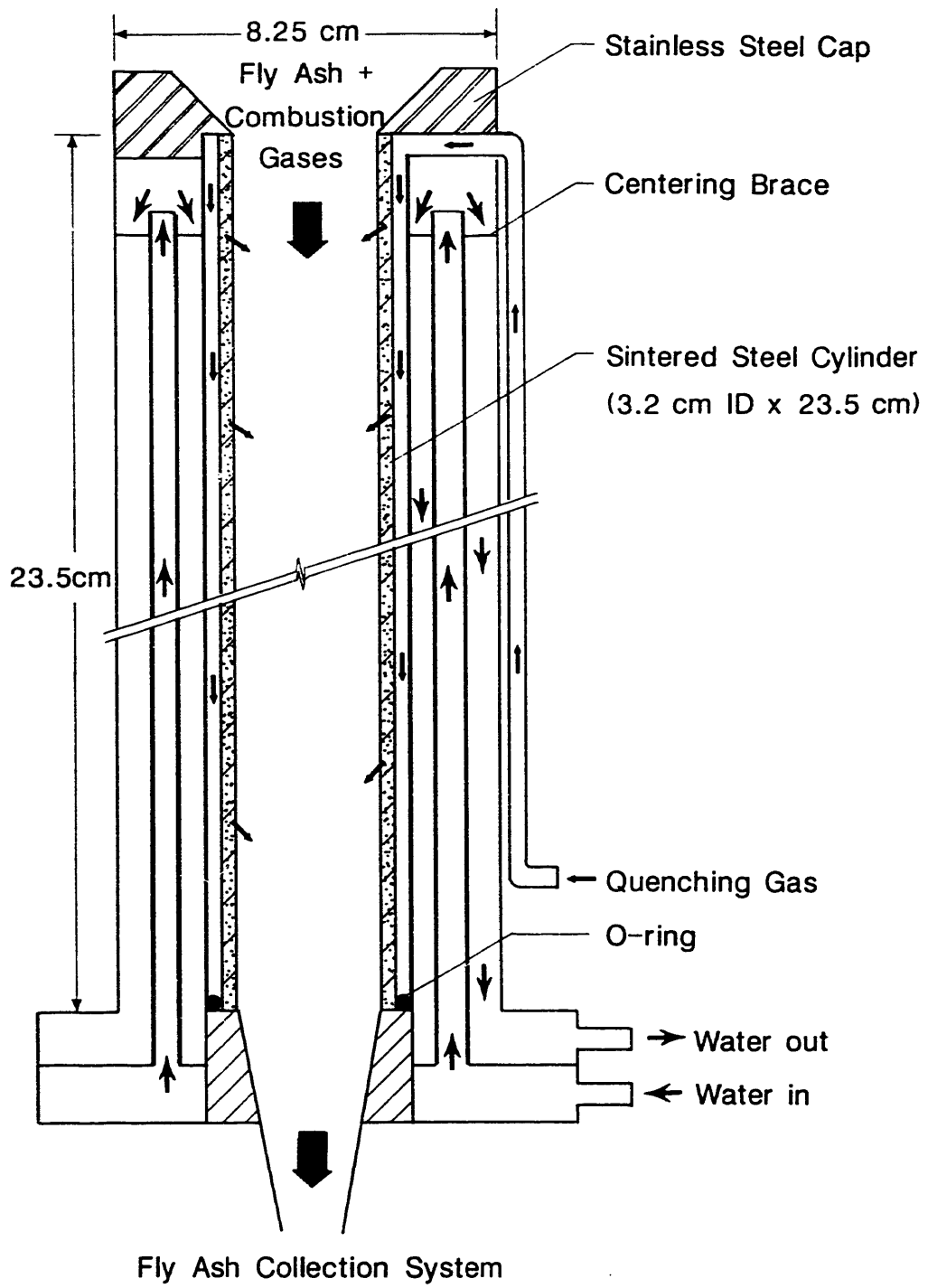

Figure 6. Fly ash quenching probe assembly for drop-tube furnace.

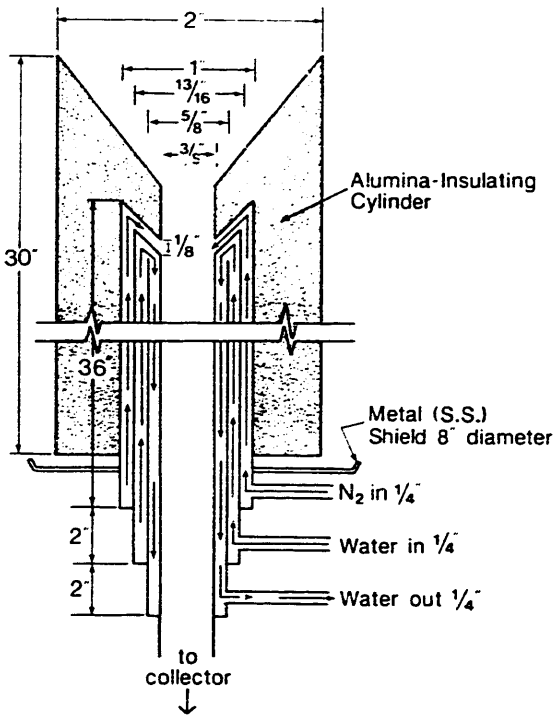

Figure 7. Short residence time probe for drop-tube furnace.

The probe is inserted in the bottom of the furnace a set distance calculated from the desired residence time. The quench gas and the vacuum are turned on. The coal is fed through the preheat injector and collected with impactor or multicyclone. The samples collected are analyzed by SEM.

4.2.2 Characterization of Coal, Char, and Fly Ash

The coals are carefully sized into three size cuts and characterized. These cuts include 38-53, 53-74, and 74-106 micrometers. Once sized, the coals are characterized by a variety of techniques to determine the abundance, size, and association of their inorganic constituents. In addition to conventional ashing followed by determination of the ash components, chemical fractionation and computer-controlled scanning electron microscopy are used to determine abundance and distributions of inorganic components as well as the size and type of mineral grains.

Chemical fractionation (6) is used to selectively extract elements from the coals based on how they are associated in the coal. Briefly, the technique involves extracting the coal with water to remove water soluble elements, followed by extraction with 1M ammonium acetate to remove elements that are associated as salts of organic acid groups. The residue from the ammonium acetate extraction is extracted with 1M HCl to remove acid soluble species in the form of organic coordination complexes, hydroxides, oxides, and carbonates. The inorganic components in the residue after all three extractions are assumed to be associated in the coal with insoluble minerals such as clays, quartz, and pyrite.

Computer-controlled scanning electron microscopy (CCSEM) is being used to characterize coal, char, and ash samples and inorganic combustion products. In addition to the CCSEM analysis of coals to determine size and type of minerals, the technique has recently been expanded to determine the juxtaposition of minerals; i.e., how minerals are associated with each other, and whether mineral grains are associated within coal particles (inherent) or associated extraneously to coal particles. This information is extremely important with respect to understanding the transformations of inorganic constituents during combustion. In order to perform such an analysis, eac' frame analyzed by CCSEM was photographed, and the coordinates of the particles were located. Inherent and extraneous associations and associations with other minerals were determined by visually examining each photograph.

4.3 Char and Fly Ash Production for Kentucky #9 and San Miguel Coals

Drop-tube furnace multicyclone and impactor tests were performed using 38-53 μm,53-74 μm, and 74-106 μm size fractions of Kentucky #9 and San Miguel coals at combustion temperatures of 1300°C, 1400°C, and 1500°C. Bulk filter tests using the 53-74 μm and bulk coal size fractions of both coals were run at combustion temperatures of 1500°C. Char production of the Kentucky #9 coal at 0.05, 0.1, 0.2, 0.5, and 0.8 second residence times also were run at combustion temperatures of 1500°C. Run conditions for the various tests are listed in Tables 4-18. The upper and lower temperatures of furnace #1 recorded in Tables 4-18 are gas temperatures derived from temperatures taken from the wall of the furnace tube. The gas temperatures have been found to be

TABLE 4
DROP-TUBE FURNACE RUN CONDITIONS FOR MULTICYCLONE COLLECTION OF FLY ASH USING KENTUCKY #9 COAL (38-53 μm)

Run #	2290	2690	2890
Gas Flow Rates (L\min):			
Primary air	0.8	0.8	0.8
Secondary air	3.2	3.2	3.2
Quench Gas (N_2)	3	3	3
Vacuum	7.5	7.5	7.5
Temperatures (°C):			
Injector	867	898	928
Preheat	1050	1090	1130
Furnace 1 Upper	1292	1392	1488
Furnace 1 Lower	1312	1413	1512
Coal Burned (g)	6.75	6.37	5.92
Coal Feed Rate (g/min)	0.08	0.09	0.06
Ash Collected (g)	0.9146	0.8543	0.7723
Residence Time (sec)	2.7	2.6	2.5

TABLE 5
DROP-TUBE FURNACE RUN CONDITIONS FOR MULTICYCLONE COLLECTION
OF FLY ASH USING KENTUCKY #9 COAL (53-74 μm)

Run #	2090	2490	1290
Gas Flow Rates (L\min):			
Primary air	0.8	0.8	0.8
Secondary air	3.2	3.2	3.2
Quench Gas (N_2)	3	3	3
Vacuum	7.5	7.5	7.76
Temperatures (°C):			
Injector	871	837	932
Preheat	1050	1090	1130
Furnace 1 Upper	1292	1385	1482
Furnace 1 Lower	1312	1410	1511
Coal Burned (g)	3.83	6.48	10.49
Coal Feed Rate (g/min)	0.06	0.09	0.14
Ash Collected (g)	0.4066	0.7458	1.1419
Residence Time (sec)	2.5	2.4	2.3

TABLE 6
DROP-TUBE FURNACE RUN CONDITIONS FOR MULTICYCLONE COLLECTION
OF FLY ASH USING KENTUCKY #9 COAL (74-106 μm)

Run #	3290	3090	3490
Gas Flow Rates (L\min):			
Primary air	0.8	0.8	0.8
Secondary air	3.2	3.2	3.2
Quench Gas (N_2)	3	3	3
Vacuum	7.5	7.5	7.5
Temperatures (°C):			
Injector	860	899	931
Preheat	1050	1090	1130
Furnace 1 Upper	1291	1388	1490
Furnace 1 Lower	1313	1410	1515
Coal Burned (g)	4.05	4.73	4.67
Coal Feed Rate (g/min)	0.09	0.1	0.16
Ash Collected (g)	0.3500	0.4941	0.4697
Residence Time (sec)	2	2	1.9

TABLE 7
DROP-TUBE FURNACE RUN CONDITIONS FOR IMPACTOR COLLECTION
OF FLY ASH USING KENTUCKY #9 COAL (38-53 μm)

Run #	1990	2590	2990
Gas Flow Rates (L\min):			
Primary air	0.8	0.8	0.8
Secondary air	3.2	3.2	3.2
Quench Gas (N_2)	3	3	3
Vacuum	7.76	7.5	7.5
Temperatures (°C):			
Injector	860	833	923
Preheat	1050	1090	1130
Furnace 1 Upper	1292	1384	1489
Furnace 1 Lower	1313	1409	1514
Coal Burned (g)	6.43	6.22	4.71
Coal Feed Rate (g/min)	0.11	0.08	0.12
Ash Collected (g)	0.8357	0.8238	0.6361
Residence Time (sec)	2.7	2.6	2.5

TABLE 8
DROP-TUBE FURNACE RUN CONDITIONS FOR IMPACTOR COLLECTION
OF FLY ASH USING KENTUCKY #9 COAL (53-74 μm)

Run #	1090	2190	1390
Gas Flow Rates (L\min):			
Primary air	0.8	0.8	0.8
Secondary air	3.2	3.2	3.2
Quench Gas (N_2)	3	3	3
Vacuum	7.76	7.5	7.76
Temperatures (°C):			
Injector	865	898	937
Preheat	1050	1090	1130
Furnace 1 Upper	1308	1392	1482
Furnace 1 Lower	1329	1414	1506
Coal Burned (g)	5.28	4.51	6.46
Coal Feed Rate (g/min)	0.06	0.05	0.16
Ash Collected (g)	0.5699	0.5022	0.7195
Residence Time (sec)	2.5	2.4	2.3

TABLE 9
DROP-TUBE FURNACE RUN CONDITIONS FOR IMPACTOR COLLECTION
OF FLY ASH USING KENTUCKY #9 COAL (74-106 μm)

Run #	3390	3190	3590
Gas Flow Rates (L\min):			
Primary air	0.8	0.8	0.8
Secondary air	3.2	3.2	3.2
Quench Gas (N_2)	3	3	3
Vacuum	7.5	7.76	7.76
Temperatures (°C):			
Injector	861	900	928
Preheat	1050	1090	1130
Furnace 1 Upper	1288	1389	1489
Furnace 1 Lower	1309	1415	1517
Coal Burned (g)	3.4	4.8	4.58
Coal Feed Rate (g/min)	0.1	0.08	0.09
Ash Collected (g)	0.3039	0.5106	0.4182
Residence Time (sec)	2	2	1.9

TABLE 10
DROP-TUBE FURNACE RUN CONDITIONS FOR BULK FILTER COLLECTION
OF FLY ASH USING KENTUCKY #9 COAL

Run #	0889	0990
Description	53-74 μm	Bulk
Gas Flow Rates (L\min):		
Primary air	0.8	0.8
Secondary air	3.2	3.2
Quench Gas (N_2)	3	3
Vacuum	7.76	7.76
Temperatures (°C):		
Injector	935	939
Preheat	1130	1130
Furnace 1 Upper	1491	1476
Furnace 1 Lower	1518	1503
Coal Burned (g)	2.96	3.07
Coal Feed Rate (g/min)	0.05	0.1
Ash Collected (g)	0.2289	0.3031
Residence Time (sec)	2.3	2.3

TABLE 11
DROP-TUBE FURNACE RUN CONDITIONS FOR CHAR PRODUCTION
USING KENTUCKY #9 COAL (53-74 μm)

Run #	0789	0689	0589	3790	3690
Gas Flow Rates (L\min):					
Primary air	0.8	0.8	0.8	0.8	0.8
Secondary air	3.2	3.2	3.2	3.2	3.2
Quench Gas (N_2)	3	3	3	3	3
Vacuum	7.76	7.76	7.76	7.5	7.5
Temperatures (°C):					
Injector	933	932	930	928	928
Preheat	1130	1130	1130	1130	1130
Furnace 1 Upper	1480	1481	1484	1497	1499
Furnace 1 Lower	1493	1494	1495	1499	1483
Coal Burned (g)	3.38	2.74	2.75	2.08	2.36
Coal Feed Rate (g/min)	0.11	0.06	0.07	0.04	0.05
Ash Collected (g)	0.3697	0.3926	0.4687	0.2312	0.2650
Residence Time (sec)	0.05	0.1	0.2	0.5	0.8

TABLE 12
DROP-TUBE FURNACE RUN CONDITIONS FOR MULTICYCLONE COLLECTION
OF FLY ASH USING SAN MIGUEL COAL (38-53 μm)

Run #	0590	0390	0190
Gas Flow Rates (L\min):			
Primary air	0.8	0.8	0.8
Secondary air	3.2	3.2	3.2
Quench Gas (N_2)	3	3	3
Vacuum	7.5	7.5	7.5
Temperatures (°C):			
Injector	858	897	929
Preheat	1050	1090	1130
Furnace 1 Upper	1290	1389	1492
Furnace 1 Lower	1313	1413	1519
Coal Burned (g)	5.1	4.75	4.69
Coal Feed Rate (g/min)	0.19	0.19	0.19
Ash Collected (g)	2.0114	1.5003	0.8940
Residence Time (sec)	2.7	2.6	2.5

TABLE 13
DROP-TUBE FURNACE RUN CONDITIONS FOR MULTICYCLONE COLLECTION
OF FLY ASH USING SAN MIGUEL COAL (53-74 μm)

Run #	1290	1590	1890
Gas Flow Rates (L\min):			
Primary air	0.8	0.8	0.8
Secondary air	3.2	3.2	3.2
Quench Gas (N_2)	3	3	3
Vacuum	7.5	7.5	7.5
Temperatures (°C):			
Injector	835	893	925
Preheat	1050	1090	1130
Furnace 1 Upper	1297	1400	1486
Furnace 1 Lower	1305	1410	1500
Coal Burned (g)	5.07	4.29	4.84
Coal Feed Rate (g/min)	0.2	0.17	0.19
Ash Collected (g)	1.8930	1.7830	2.1392
Residence Time (sec)	2.5	2.4	2.3

TABLE 14
DROP-TUBE FURNACE RUN CONDITIONS FOR MULTICYCLONE COLLECTION
OF FLY ASH USING SAN MIGUEL COAL (74-106 μm)

Run #	1790	1090	0890
Gas Flow Rates (L\min):			
Primary air	0.8	0.8	0.8
Secondary air	3.2	3.2	3.2
Quench Gas (N_2)	3	3	3
Vacuum	7.5	7.5	7.5
Temperatures (°C):			
Injector	860	886	922
Preheat	1050	1090	1130
Furnace 1 Upper	1290	1407	1492
Furnace 1 Lower	1305	1417	1519
Coal Burned (g)	4.69	3.57	4.64
Coal Feed Rate (g/min)	0.24	0.19	0.19
Ash Collected (g)	0.2760	0.0605	0.4891
Residence Time (sec)	2	2	1.9

TABLE 15
DROP-TUBE FURNACE RUN CONDITIONS FOR IMPACTOR COLLECTION
OF FLY ASH USING SAN MIGUEL COAL (38-53 μm)

Run #	0690	0490	0290
Gas Flow Rates (L\min):			
Primary air	0.8	0.8	0.8
Secondary air	3.2	3.2	3.2
Quench Gas (N_2)	3	3	3
Vacuum	7.5	7.5	7.5
Temperatures (°C):			
Injector	854	893	925
Preheat	1050	1090	1130
Furnace 1 Upper	1292	1389	1490
Furnace 1 Lower	1315	1414	1517
Coal Burned (g)	0.85	0.84	1.52
Coal Feed Rate (g/min)	0.14	0.17	0.15
Ash Collected (g)	0.2828	0.2761	0.5698
Residence Time (sec)	2.7	2.6	2.5

TABLE 16
DROP-TUBE FURNACE RUN CONDITIONS FOR IMPACTOR COLLECTION
OF FLY ASH USING SAN MIGUEL COAL (53-74 μm)

Run #	1390	1490	1990
Gas Flow Rates (L\min):			
Primary air	0.8	0.8	0.8
Secondary air	3.2	3.2	3.2
Quench Gas (N_2)	3	3	3
Vacuum	7.5	7.5	7.5
Temperatures (°C):			
Injector	834	892	923
Preheat	1050	1090	1130
Furnace 1 Upper	1298	1394	1487
Furnace 1 Lower	1308	1406	1500
Coal Burned (g)	0.78	0.89	0.9
Coal Feed Rate (g/min)	0.2	0.25	0.23
Ash Collected (g)	0.2798	0.3249	0.3980
Residence Time (sec)	2.5	2.4	1.9

TABLE 17
DROP-TUBE FURNACE RUN CONDITIONS FOR IMPACTOR COLLECTION
OF FLY ASH USING SAN MIGUEL COAL (74-106 μm)

Run #	1690	0990	1790
Gas Flow Rates (L\min):			
Primary air	0.8	0.8	0.8
Secondary air	3.2	3.2	3.2
Quench Gas (N_2)	3	3	3
Vacuum	7.5	7.5	7.5
Temperatures (°C):			
Injector	865	881	926
Preheat	1050	1090	1130
Furnace 1 Upper	1290	1392	1492
Furnace 1 Lower	1303	1416	1518
Coal Burned (g)	0.95	0.83	0.91
Coal Feed Rate (g/min)	0.24	0.21	0.18
Ash Collected (g)	0.1752	0.0845	0.1051
Residence Time (sec)	2	2	1.9

TABLE 18
DROP-TUBE FURNACE RUN CONDITIONS FOR BULK FILTER COLLECTION
OF FLY ASH USING SAN MIGUEL COAL

Run #	2090	2190
Description	53-74 μm	Bulk
Gas Flow Rates (L\min):		
Primary air	0.8	0.8
Secondary air	3.2	3.2
Quench Gas (N_2)	3	3
Vacuum	7.5	7.5
Temperatures (°C):		
Injector	927	923
Preheat	1130	1130
Furnace 1 Upper	1483	1486
Furnace 1 Lower	1497	1500
Coal Burned (g)	0.85	1.79
Coal Feed Rate (g/min)	0.17	0.18
Ash Collected (g)	0.3136	0.6931
Residence Time (sec)	3.9	3.9

approximately 30°C lower than the wall temperatures by tests performed with a suction pyrometer.

4.4 Fly Ash Particle-Size and Composition Evolution

Introduction

Particle-size distributions of minerals and amorphous phases were determined using CCSEM for Combustion Inorganic Transformation (CIT) test coals and chars, including the Beulah lignite and Upper Freeport. Data produced on the chars were obtained by analyzing whole grain mounts of the chars on double-stick tape. The results were checked using cross-sectioned char mounts producing the same overall particle-size distribution number percent results. The number of mineral particles in each of the following size categories was determined: <1.2, 1.2-2.1, 2.1-4.4, 4.4-8.0, 8.0-11.0, and >11.0 microns. This information provides a basis for understanding the fragmentation or coalescence of minerals during combustion of these test coals.

More detailed analysis was made of the Beulah and Upper Freeport coal, char, and fly ash inorganics by observing weight percent concentrations of inorganics in different size categories. Total inorganic particles were plotted versus size using a geometric size distribution in order to observe the overall distribution particles greater than 11 microns. In addition, weight percent concentrations of selected minerals that were being transformed or produced with time during the combustion process were plotted as a function of size. In effect this gives a time-resolved look at inorganic transformations. Using this information, the interaction of different minerals and inorganics was described and inferred.

The end result of this approach to studying fly ash is that particle size and composition evolution with time can be observed through time, and this information is helpful input into models which attempt to predict fly ash size and composition.

Beulah

The whole grain mount analysis of Beulah char phases produced at selected residence times revealed that greater quantities of larger-sized particles were formed during char formation as compared to the original mineral size distribution observed in the coal (Figure 8). This is apparent evidence for coalescence of smaller inorganic particles to form larger ones. Analysis of the cross-sectioned chars revealed similar number percent distributions of Beulah fly ash particles, indicating coalescence with time (Figure 9). Comparison of cross-sectioned coal minerals, ash particles in 0.5 and 0.8-second char ash particles, and 100% carbon burnout fly ash particles was performed on a weight percent basis as shown in Figure 10. Residence time for the fly ash was about 1.5 seconds. Coalescence is evident for the inorganics, with the final fly ash showing the most mass in the >10μm fraction and the least amount of material in the <10μm range.

Quartz was reduced in quantity with time, showing an almost even degradation (Figure 11). The reduction is primarily the result of reaction, with Na and

Ca coming out of the organic bonding sites in the coal matrix. Calcium silicate, which was nonexistent in the coal, comprised nearly 4% of the ash at 0.8 seconds. Sodium silicates appear to form only as a skin on quartz particles. Although no CCSEM category currently exists to classify sodium silicate, examination of the data found that approximately 1% of the quartz grains contained 2% or more sodium. Previous work revealed the presence of Na-rich sulfates and silicates mainly on the surface layers of Beulah chars and fly ash (7,8).

Aluminosilicates derived from clay minerals such as kaolinite and halloysite reacted pervasively with organically bound Na and Ca. The most obvious evidence for this conclusion is the production of calcium aluminosilicate with time as shown in Figure 12. Reaction of CaO with aluminosilicates appears to be especially promulgated among the smaller-sized clay grains (<10μm) which are more intimately associated with the organic matrix and, though small, comprise a large reactive surface area. Figure 12 reveals that calcium aluminosilicates, which are virtually nonexistent in the coal, are more abundant in the smaller size ranges of char during early combustion, but with time coalesce to form particles that are mostly greater than 10 microns in average diameter. A plot of the aluminosilicate distribution with time, given in Figure 13, shows that initially the clays are abundant in the smaller size ranges, but upon combustion the concentrations in the smaller size ranges decrease dramatically with an increase in larger-sized grains. This is evidence again for the interaction between organically bound Ca and aluminosilicate to transform mineral aluminosilicates such as kaolinite to calcium aluminosilicates during combustion.

Reaction of sodium with clay minerals is also evident from the CCSEM data. Figure 14 illustrates that Na may have a similar reactivity with the clays as Ca does because they have concentrations that are somewhat proportional. The 0.8-second char contained about 5% Na-bearing aluminosilicates, the Na being at least 3% or more of the particle, based on CCSEM EDS levels. Approximately 2% of the 0.8-second char also consisted of Na-bearing calcium aluminosilicates, again with the sodium being at least 3% of the EDS particle composition.

Pyrite is a major constituent in the Beulah coal, comprising 26% of the coal minerals. Upon combustion, the content of pyrite decreases dramatically as displayed in Figure 15. This would be expected since pyrite readily converts to pyrrhotite and then to forms of iron oxide beginning at temperatures as low as 500°C (9). Indeed iron oxide, which was not present in the coal, was detected by CCSEM in the chars (Figure 16). The sizes of the iron oxide particles were similar to those observed for the pyrite, except there is a slight increase in material noted in the 4.6-10 μm category which may be evidence for fragmentation of pyrite.

Upper Freeport

The particle-size distribution for mineral phases in the Upper Freeport chars (Figure 17) shows an initial increase in the number of particles in the smaller size categories. By 0.8 seconds, however, larger quantities of phases are found in the >11.0 μm fraction than in the coal. Weight percent distributions present evidence of coalescence of inorganic ash particles with quantities of minerals being reduced in the <10μm range and increased in the 22-48 μm range with time (Figure 18). These trends may indicate that initially fragmentation of

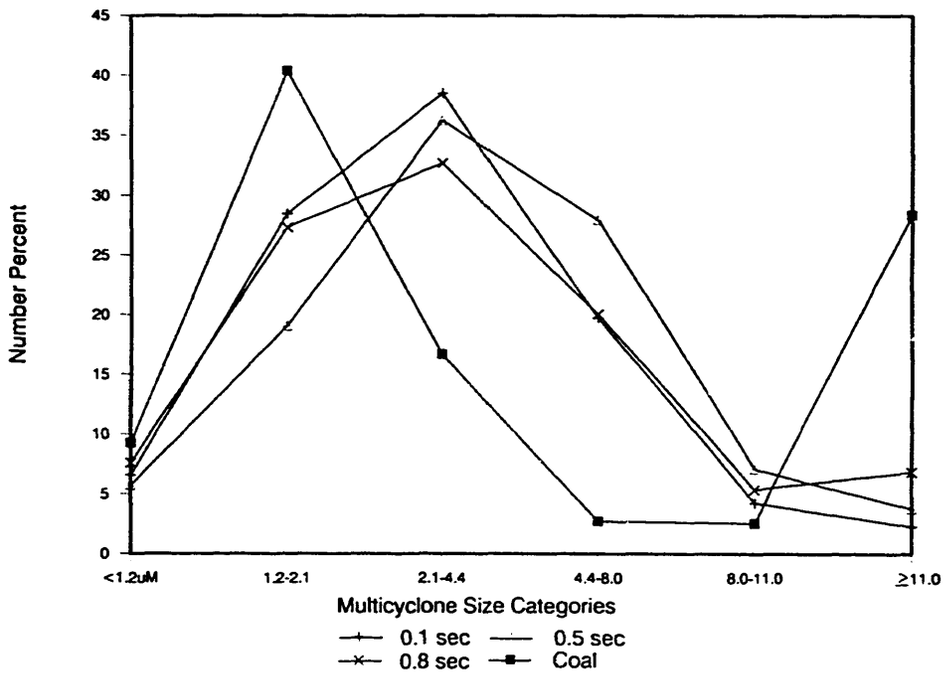

Figure 8. Whole-grain mount particle-size distribution of Beulah coal and char phases.

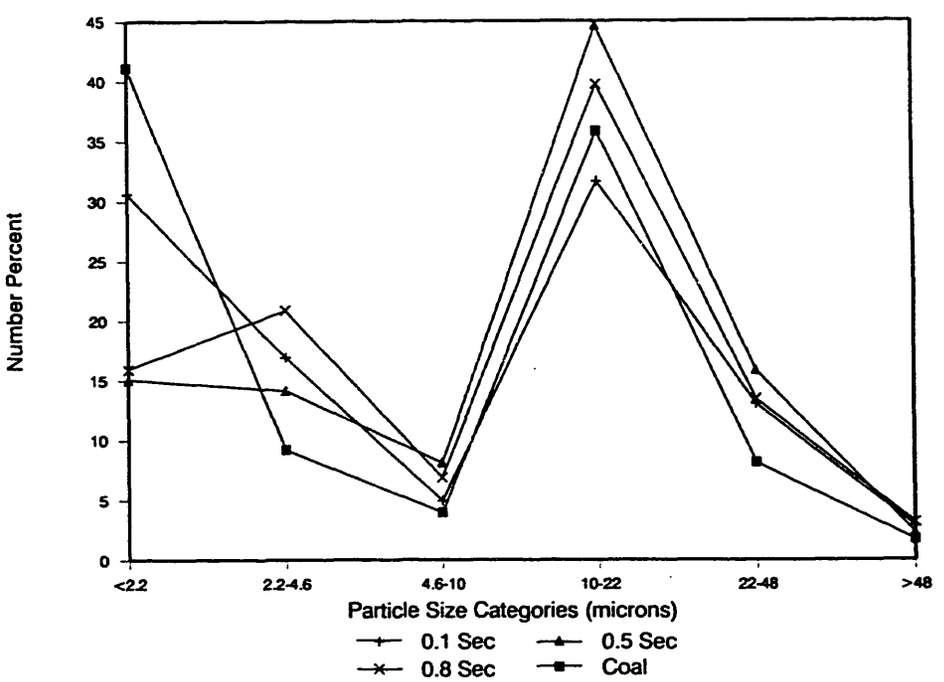

Figure 9. Cross-section particle-size distribution of Beulah coal and char phases.

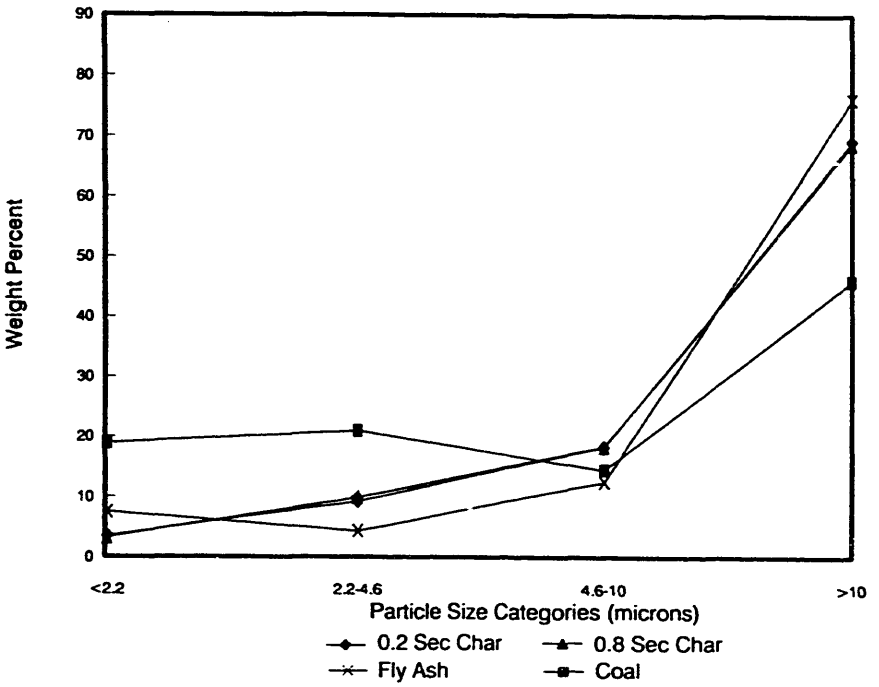

Figure 10. Cross-section particle-size distribution of Beulah coal minerals, char phases and fly ash.

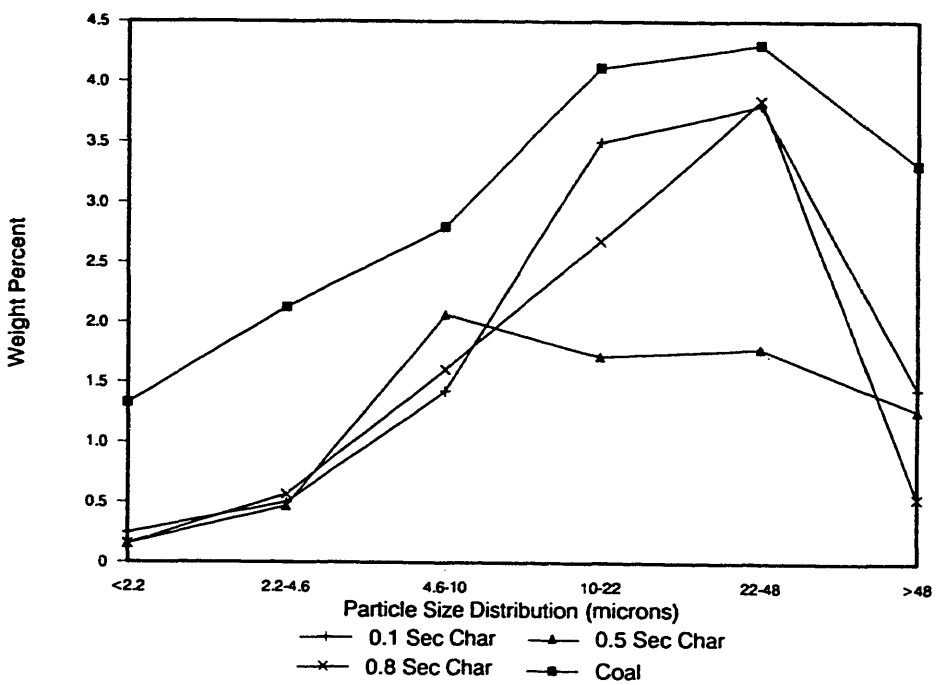

Figure 11. Distribution of quartz in Beulah coal and chars during combustion.

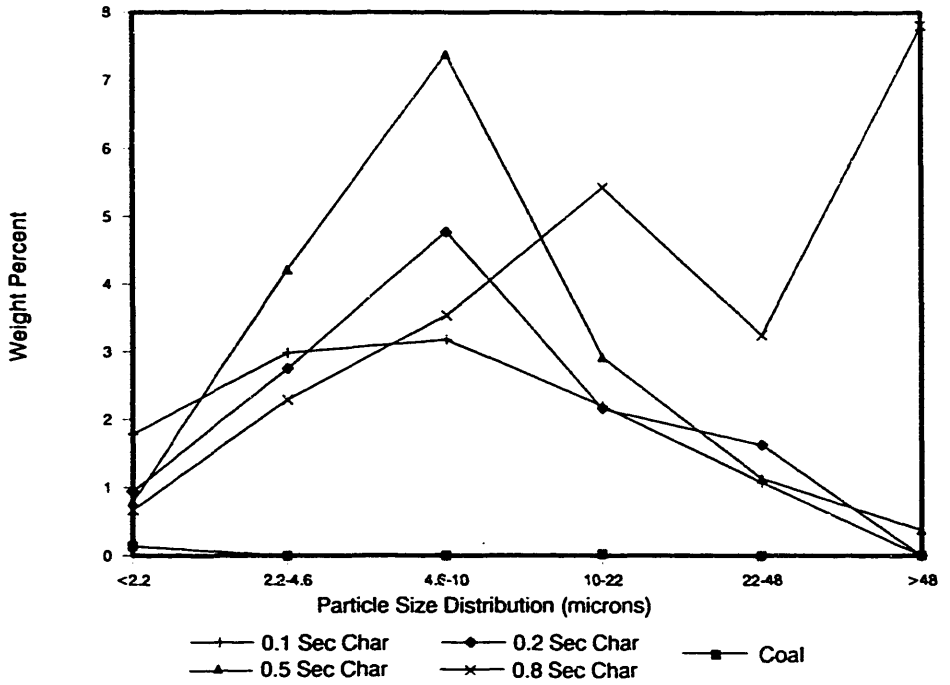

Figure 12. Distribution of Ca-aluminosilicate in Beulah coal and chars during combustion.

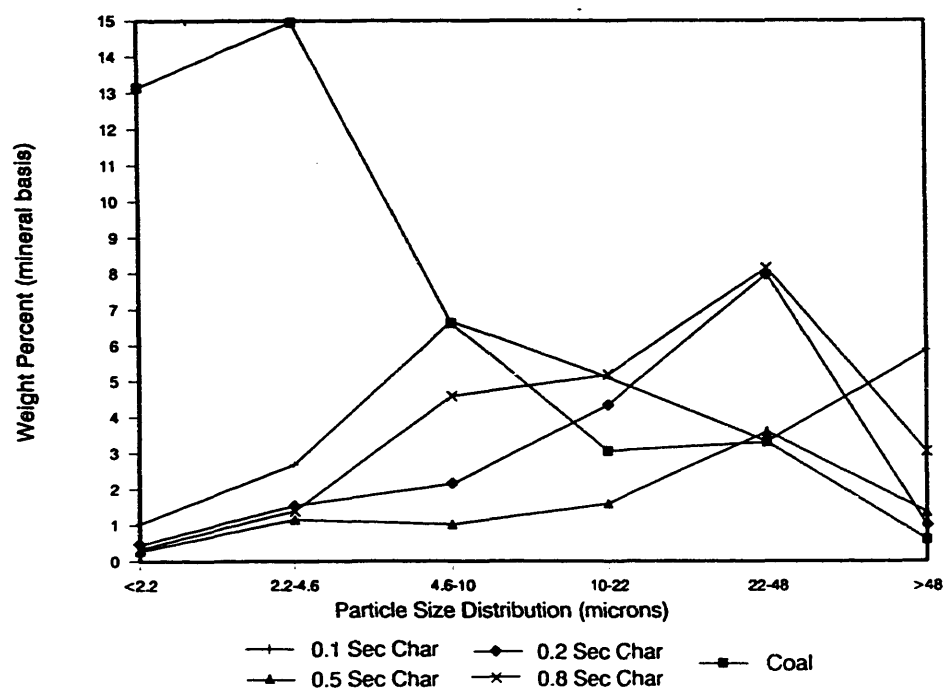

Figure 13. Distribution of aluminosilicate in Beulah coal and chars during combustion.

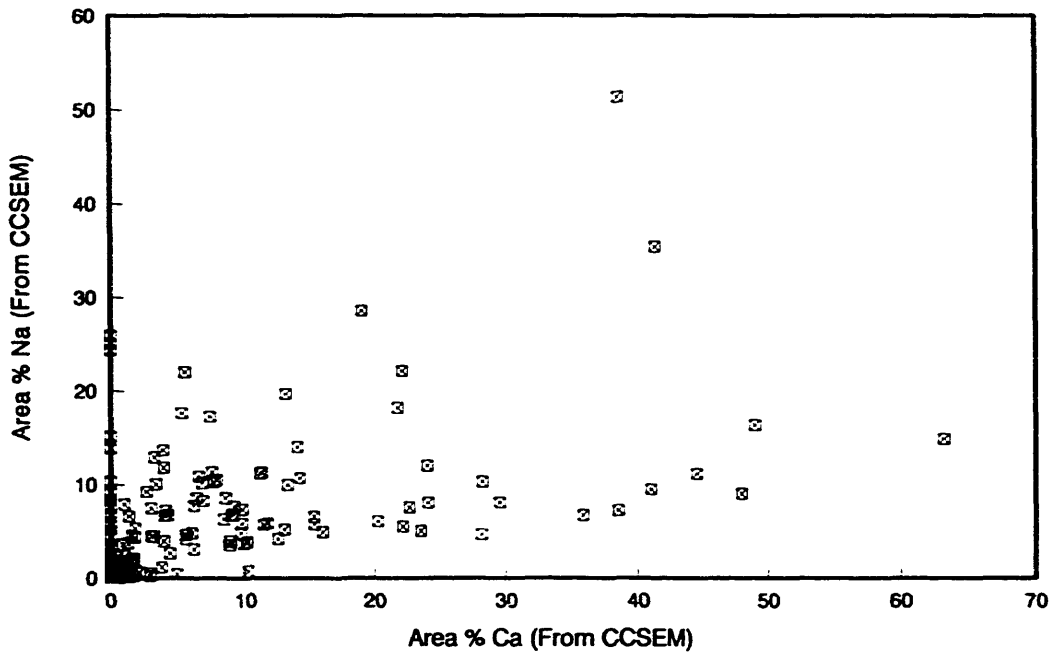

Figure 14. Scatter plot of Na quantity as a function of Ca quantity in Beulah fly ash aluminosilicates.

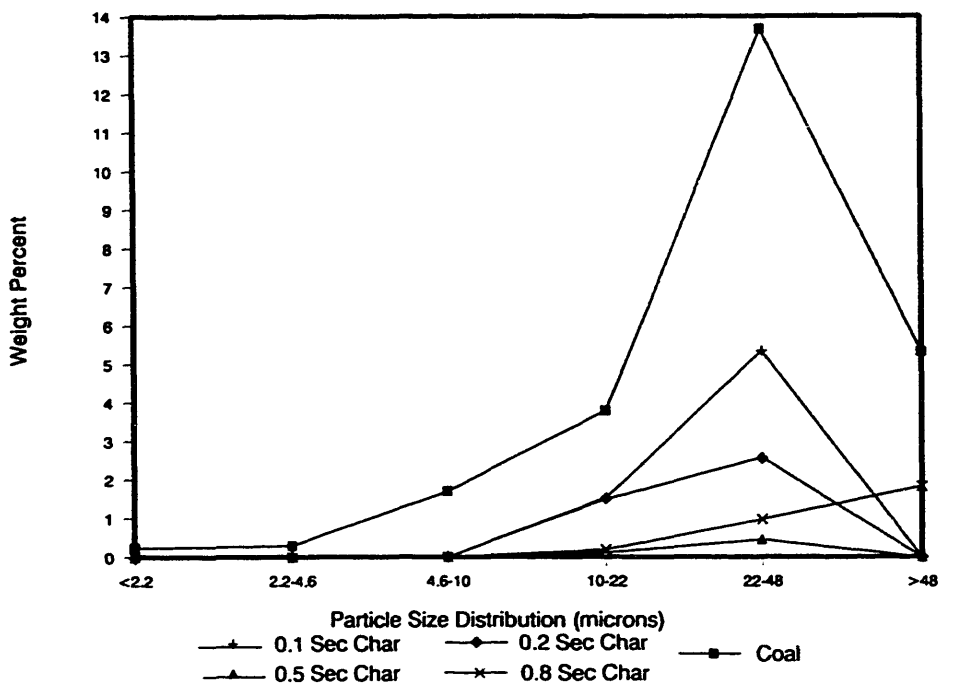

Figure 15. Distribution of pyrite in Beulah coal and chars during combustion.

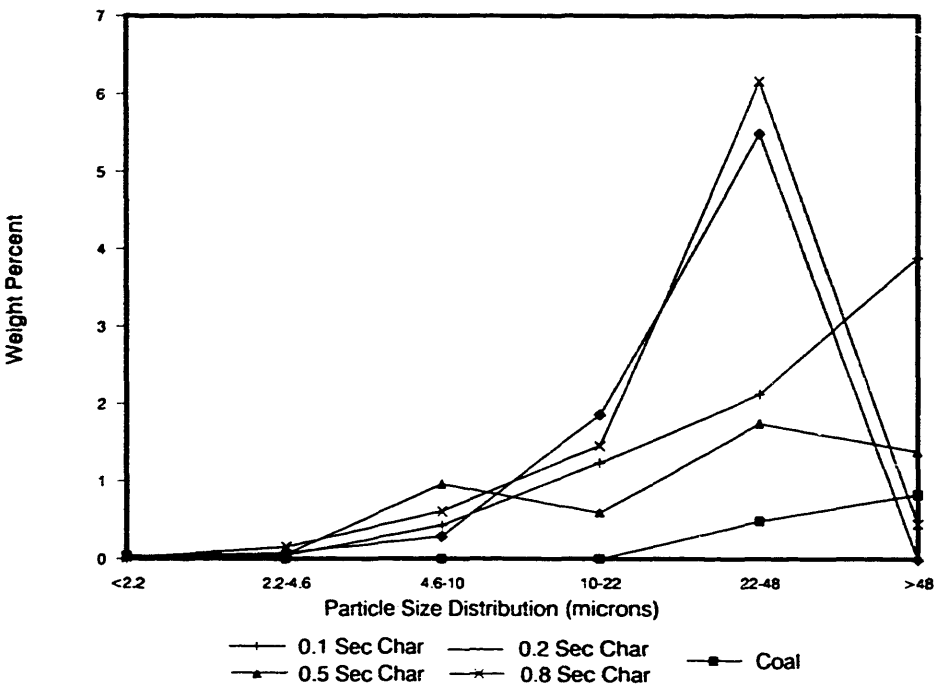

Figure 16. Distribution of iron oxide in Beulah coal and chars during combustion.

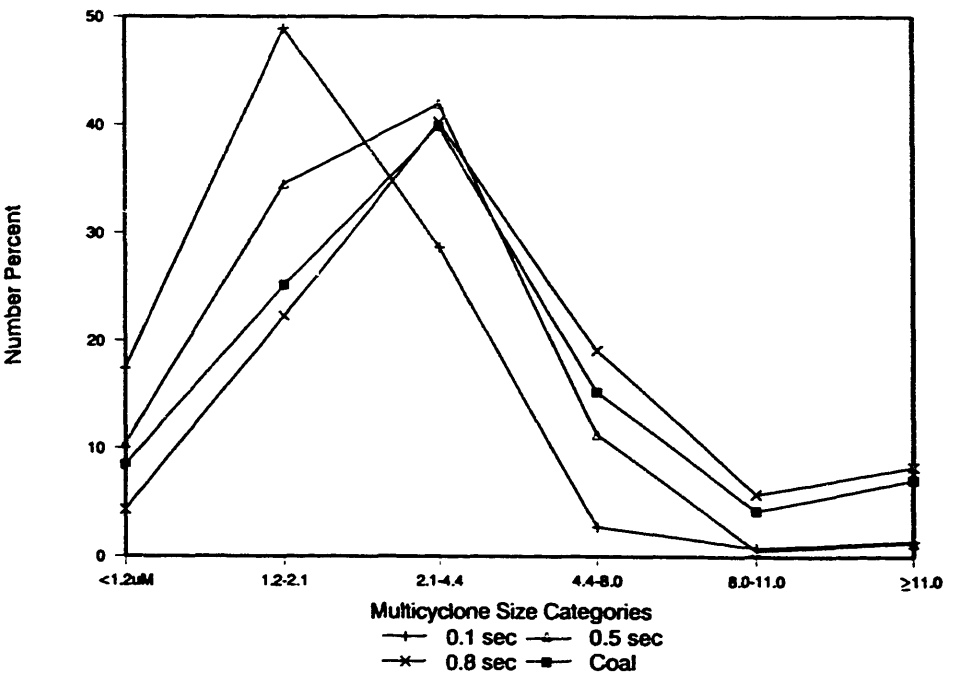

Figure 17. Cross-section particle-size distribution of Upper Freeport coal and char phases during combustion.

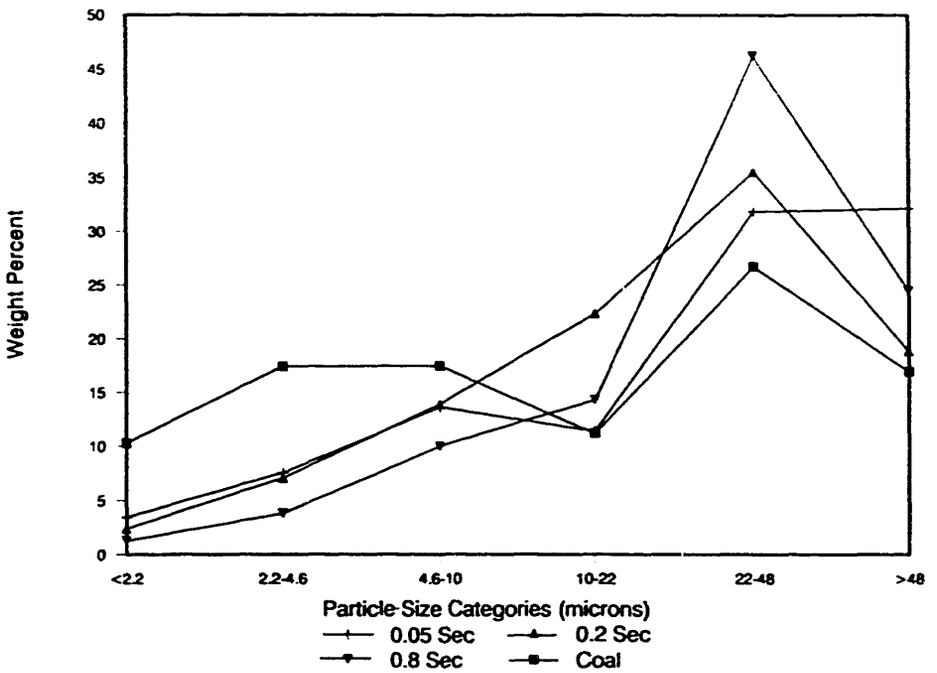

Figure 18. Cross-section particle-size distribution of Upper Freeport coal and char phases.

mineral grains may be occurring with subsequent coalescence of ash particles as the combustion process proceeds.

Iron aluminosilicates have often been associated with wall slagging in boilers that fire bituminous coals such as the Upper Freeport; therefore, the formation of this phase is of prime interest. Figure 19 indicates that iron aluminosilicate particles were produced in the char mostly in the 22-48 μm size range. Some coalescence of existing iron aluminosilicate minerals in the coal may have occurred also. Sources of Fe and aluminosilicate material for the additional iron aluminosilicate phases produced were probably pyrite or iron oxide for Fe and kaolinite or illite for the aluminosilicate. Iron is also present in the illite, reaching levels of 5% of the illite chemical composition.

Illite was originally bimodally distributed in the Upper Freeport coal at 2.2-4.6 μm and 22-48 μm, but upon combustion, the smaller illite grains coalesced forming a unimodal distribution about the median of 22-48 μm (Figure 20). The shift of material from the smaller size ranges does not completely correlate or compensate in crude mass balance with the increase at the larger size range, implying that production of K-aluminosilicate may have occurred by reaction between illite and aluminosilicate, minerals such as kaolinite.

Pyrite decomposed to iron oxide in much the same manner as with the Beulah, except that by 0.8 seconds the pyrite composition was either completely destroyed or unrecognized by CCSEM (Figures 21 and 22). The iron oxide quantities produced (Figure 22) do not account for all the released iron from the pyrite. This may indicate that some of the released iron oxide has by this time reacted with aluminosilicate to form iron aluminosilicate.

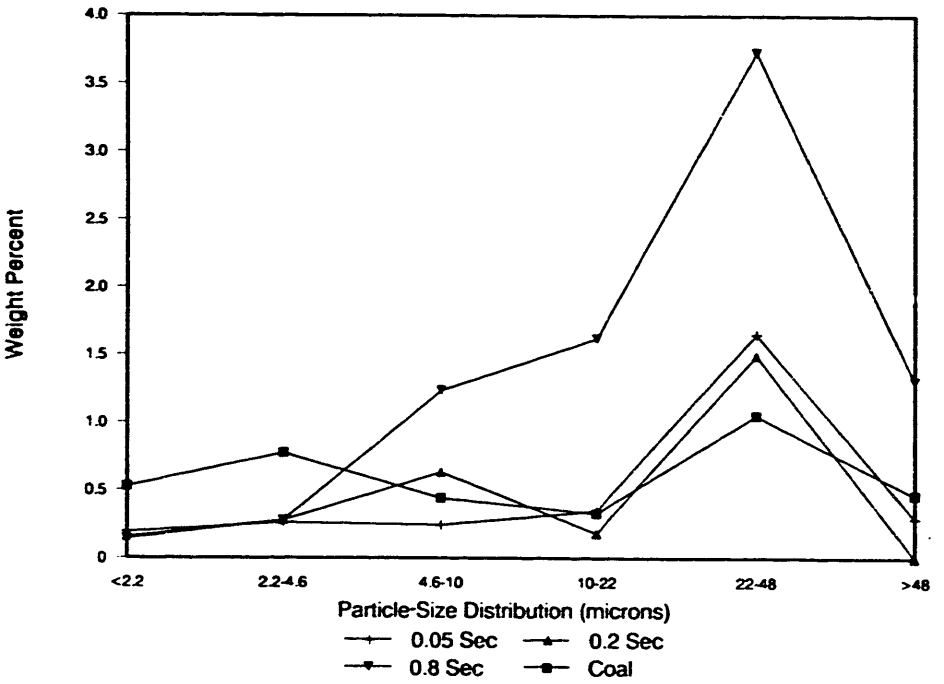

Figure 19. Distribution of Fe-aluminosilicate in Upper Freeport coal and char during combustion.

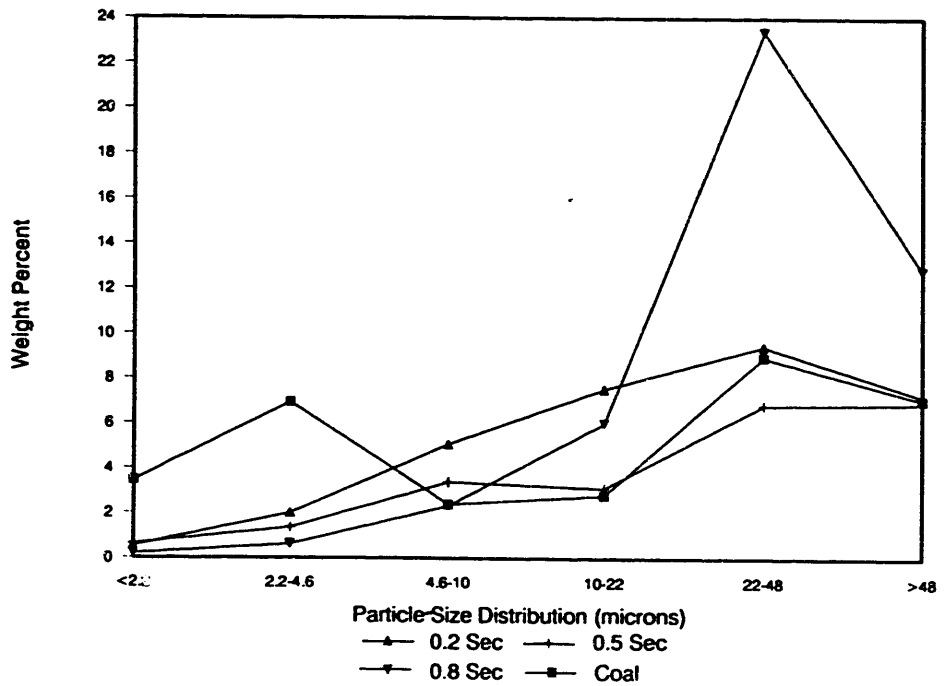

Figure 20. Distribution of illite or K-aluminosilicate in Upper Freeport coal and char during combustion.

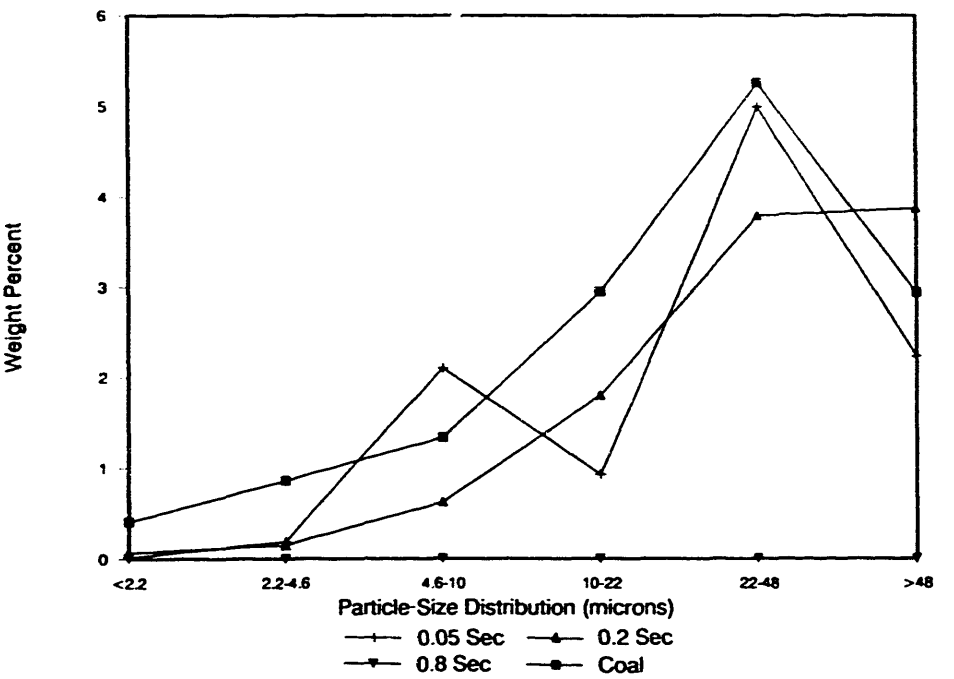

Figure 21. Distribution of pyrite in Upper Freeport coal and char during combustion.

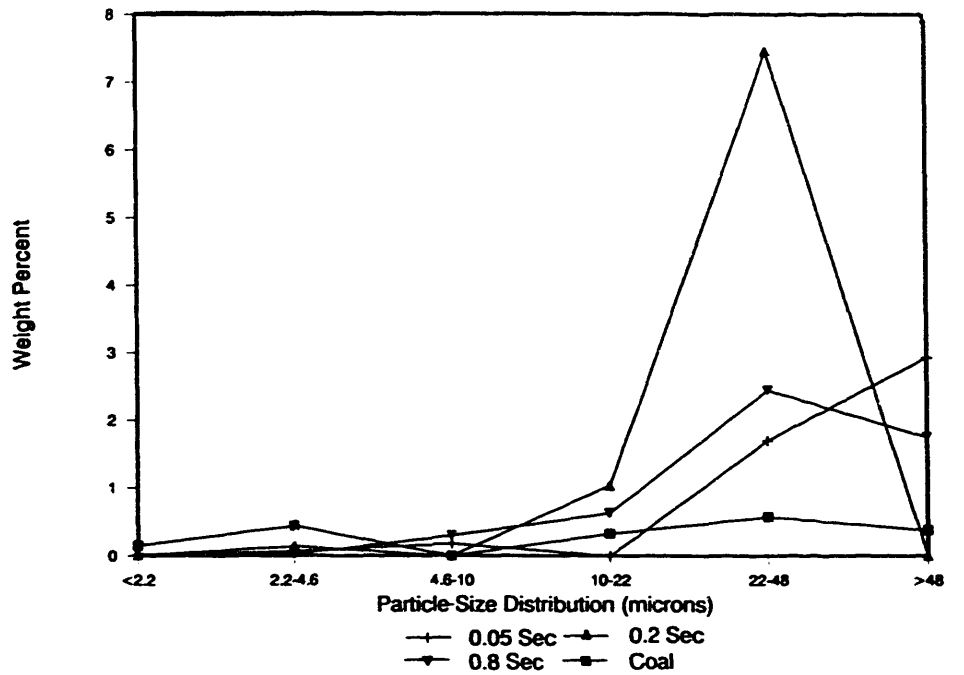

Figure 22. Distribution of iron oxide in Upper Freeport coal and char during combustion.

4.3 Summary and Conclusions

Combustion testing of Kentucky #9 and San Miguel coals in the drop-tube furnace was nearly completed. Fly ash was generated at three temperatures for three different size fractions of both coals and collected using both the multicyclone and impactor. Bulk fly ash samples were also collected on a filter for the unsized and 53-74μm coal feeds. Short residence time chars were generated for the Kentucky #9. All of the samples were submitted for analysis using either CCSEM or scanning electron microscopy point count (SEMPC).

Particle-size distributions of discrete mineral or amorphous phases in intermediates produced in the drop-tube furnace (DTF) for two coals were examined. Time-resolved PSD's of phases show that Beulah and Upper Freeport inorganic phases coalesce with time. The Upper Freeport shows an initial increase in the amounts of particles in the smaller size ranges due to fragmentation of minerals or the formation of smaller inorganic ash droplets from submicron minerals or inorganics. The transformation of selected inorganic components through time was also noted. Sodium and calcium organically associated in the Beulah react readily with smaller-sized kaolinitic clays and, to a much lesser degree, with quartz. Pyrite appears to undergo fragmentation during combustion in the Beulah and Upper Freeport, with a resulting increase in iron oxide. Iron aluminosilicates in Upper Freeport ash is probably the result of Fe from decomposed pyrite reacting with aluminosilicate clay material such as illite and kaolinite.

5.0 REFERENCES

1. Kalmanovitch, D.P.; Frank, M. "An Effective Model of Viscosity for Ash Deposition Phenomena"; Presented at the Conference on Mineral Matter and Ash Deposition from Coal, The Engineering Foundation, Santa Barbara, California, February 21-26, 1988.

2. Ramanathan, M.; Kalmanovitch, D.P.; Ness, S. "New Techniques for Thermochemical Phase Equilibria Prediction in Coal Ash Systems II: High Temperature Materials Chemistry, 89"; Sixth International Conference on High Temperatures - Chemistry of Inorganic Materials, Gaithersburg, Maryland, April 3-7, 1989.

3. Zygarlicke, C.J.; Benson, S.A.; Hurley, J.P., and Steadman, E.N. "Combustion Inorganic Transformations"; Fifteenth Quarterly Technical Progress Report for the period October to December 1989, DE-FC21-86MC10637.

4. "Program Plan for Transformations of Inorganic Coal Constituents in Combustion Systems"; Prepared by A.A. Boni, Physical Sciences, Inc., 1986, DE-AC22-86PC90751, 1987.

5. Kalmanovitch, D.P., Montgomery, G.G.; and Steadman, E.N. ASME Paper Number 87-JPGC-FACT-4.

6. Benson, S.A., Holm. P.L. Ind. Eng. Chem Prod. Res. Dev., 1985, 145-149.

7. "Combustion Inorganic Transformations"; Fourteenth Quarterly Technical Progress Report for the period July to September 1989, DE-FC21-86MC10637.

8. "Combustion Inorganic Transformations"; Final Report for the period April 1988 to June 1989, DE-FC21-86MC10637.

9. Watt, J.D. "The Physical and Chemical Behavior of the Mineral Matter in Coal Under Conditions Met in Combustion Plant: Pt. II"; Leatherhead, Surrey: BCURA Industrial Laboratories, Aug. 1969.

3.3 (Combined with Section 3.2)

3.4 Liquefaction Reactivity of Low-Rank Coals

LIQUEFACTION REACTIVITY OF LOW-RANK COALS

Quarterly Technical Progress Report
for the Period January - March 1990

by

Edwin S. Olson, Research Supervisor
Energy & Environmental Research Center
University of North Dakota
P.O. Box 8213, University Station
Grand Forks, ND 58202

Contracting Officer's Technical Representative: Udaya Rao

for

U.S. Department of Energy
Pittsburgh Energy Technology Center
Pittsburgh, Pennsylvania 15236

May 1990

Work Performed Under Cooperative Agreement No. DE-FC21-86MC10637

TABLE OF CONTENTS

LIST OF FIGURES

LIST OF TABLES

LIQUEFACTION REACTIVITY OF LOW-RANK COALS

1.0 EXECUTIVE SUMMARY

Further characterization of silica gel zinc chloride catalyst was carried out to provide further information on the nature of this solid acid catalyst. Total acidity and type of acidity of this catalyst were determined by infrared spectroscopy and thermogravimetric analysis of the pyridine-absorbed catalyst. Acidity studies showed that the silica gel zinc chloride catalyst contains significant numbers of highly acidic sites. The number of Lewis acid sites are almost three times the number of Brönsted acid sites.

The reactions of silica gel zinc chloride catalyst with 1- and 2-methylnaphthalenes have been investigated at several time intervals to provide suitable mechanistic models for coal liquefaction. During short reaction times (5-60 minutes), isomerization of 1- or 2-methylnaphthalenes was the major reaction, but at longer reaction times (3-24 hours), hydrogenation, dealkylation, and hydrocracking occurred readily.

Reactions of bibenzyl were investigated to establish the role of molecular hydrogen in the acid-catalyzed cleavage reactions. Although cleavage reactions and reduced products were obtained in the absence of hydrogen, the presence of hydrogen is necessary to avoid coking and to improve the product yield. The results are interpreted to mean that hydrogen reduces some of the condensation products, converting them to better hydride donors. Thus the condensation products will be effectively involved in the primary reactions that give ethylbenzene, rather than progressively lose hydrogen and form coke.

Further substantiation and elaboration of the acid-catalysis mechanisms were undertaken. The reaction of diphenylpropane gave high conversion to benzene and indan, implicating free carbonium ion intermediates. With neopentylbenzene, the conversion was low, and the major products were benzene and 2-methylbutane from rearrangement of the neopentyl carbonium ion. These products are suggestive of Brönsted acid catalytic sites. Toluene, 2-methylpropane, and other linear alkanes indicated the possible involvement of the Lewis acid sites.

2.0 GOALS AND OBJECTIVES

The efficient production of environmentally acceptable distillate fuels requires catalysts for hydrogenation and cleavage of the coal macromolecules and removal of oxygen, nitrogen, and sulfur heteroatoms. Currently, two-stage processes for coal conversion are under development. The first stage converts coal to a soluble form with minimal cracking and hydrogenation. This processing presently involves no catalyst other than the coal mineral matter present and addition of a promoter, hydrogen sulfide, which may have a catalytic effect. The second stage involves hydrogenation upgrading of the first-stage product to distillates with fixed- or ebullated-bed catalysts.

The catalysts currently used in the second stage of coal liquefaction for hydrotreating the first-stage product are the same as those used in conventional petroleum refining; however, this application has not been very successful. Improvements in upgrading efficiency could be obtained if catalysts with longer life and better activity and selectivity were available. Rapid deactivation of the conventional Co-Mo and Ni-Mo catalysts on an alumina support have been attributed to coke formation, metals deposition, and inhibition of the active center by chemisorbed compounds.

The objectives of this research project are to develop and test novel heterogeneous catalysts for hydrotreatment upgrading of first-stage coal liquefaction products. The new hydrogenation catalysts are based on pillared clays and hydrotalcites, which have very large micropore dimensions to accommodate the coal macromolecules, yet not possessing strong acidities which lead to coking at high temperatures.

A second objective is to develop a solid acid catalyst for depolymerization of coal macromolecules. The acid catalysis process for coal liquefaction is believed to operate by ionic mechanisms. Some molten acids have successfully depolymerized coal, but the poor efficiencies of catalyst recovery and the corrosive nature of the catalyst make the process uneconomical. Stable solid acid catalysts will be developed which will avoid these difficulties. These catalysts are also based on pillared clays as well as a silica bases.

3.0 ACCOMPLISHMENTS

3.1 Introduction

The development of new heterogeneous catalysts for hydrotreating was continued. The synthesis of several new catalysts was accomplished. The new catalysts are basically of two types, sulfided metal hydrogenation catalysts and solid acid ionic hydrogenation catalysts. These are discussed separately below.

3.1.1 Metal Hydrogenation Catalysts on Pillared Smectite Support

Acid smectite clays are used as catalysts in petroleum-cracking and various other reactions. Unfortunately, they dehydrate and collapse at temperatures above 200°C. Acid zeolites are more stable at high temperatures; however, the pores are too narrow to be useful for coal macromolecules, and they are not effective in upgrading as compared with conventional Ni-Mo or Co-Mo catalysts. In the pillared clays, intercalation of hydroxylated or complexed metal cations maintains the clay layer structure after loss of water and generates large pore sizes. These structures are stable to 450° and 500°C. The alumina cluster-pillared clays are effective catalysts for petroleum catalysis. Chromia-pillared clays with even larger pore spacings have considerable potential for upgrading. Wyodak coal with in situ chromia-pillared coal clays with and without incorporated hydrogenation catalysts are being prepared. Wyodak coal loaded with in situ Ni-Mo hydrogenation catalyst has also been prepared. Both these coals have been presulfided and are being tested in a two-stage coal liquefaction process.

3.1.2 Solid Acid-Catalyzed Hydrocracking

Acid-catalyzed coal conversion has been thoroughly investigated; however, the efficiencies of catalyst recovery are either not high enough or the catalyst is consumed, resulting in high cost. Another disadvantage is the corrosive nature of the catalyst. A stabile solid acid catalyst may have more potential in recovery schemes. Acid zeolites can be used at high temperatures, but have pore sizes too small for the large coal macromolecules. Thermally stabile pillared clay catalysts with large interlayer pores are more attractive for acid-catalyzed depolymerization of coal macromolecules. Chromium and aluminum cluster-pillared smectites are being tested both in the Brönsted and Lewis acid form, the latter being formed from reactions with metal chlorides. The liquefaction reactivity of Wyodak coal which has been in situ pillared with polyoxy chromium ions or metal(s)-supported will be compared with other solid acid catalysts, such as Drago aluminum chloride-silica complex and a similar zinc chloride complex. Also, reactions of silica gel-supported tin(II) chloride and zinc sulfate will be compared with silica gel zinc chloride catalyst.

3.2 Experimental

3.2.1 Catalyst Preparation

3.2.1.1 Preparation of Silica Gel Catalysts

Mixtures of silica gel with tin (II) chloride and silica gel with zinc sulfate were prepared using the same procedure as described for the preparation of silica gel zinc chloride in our previous quarterly report (1).

3.2.1.2 Preparation of In Situ Chromia-Pillared Wyodak Coal

Chromium nitrate nonhydrate (69.12 g) dissolved in 1.728 liters of deionized water was placed in a round-bottomed flask and hydrolyzed with anhydrous sodium carbonate (18.32 g). The freshly hydrolyzed chromium nitrate solution was aged at 95°C for 36 hours. At this stage, 5 g of Beulah lignite (Argonne premium coal, AR) suspended in 400 mL of deionized water (1 wt%) was added slowly at room temperature, along with vigorous stirring. The slurry was aged at room temperature for 2 hours. The solid was separated by centrifugation, and the residue was washed with deionized water until free of chromium ions. The residue was dried at 200°C.

3.2.1.3 Preparation of Bimetallic Metal-Supported Coal

A solution of nickel nitrate hexahydrate (1.07 g) and ammonium molybdate (1.51 g) in 200 mL of deionized water was placed in a 500-mL, round-bottomed flask. To this solution was added 10.0 g of Wyodak coal (Argonne premium sample, AR) and stirred overnight. The solvent was evaporated and the residue dried at 200°C

The bimetallic, metal-supported, chromia-pillared Wyodak coal was prepared in the same manner.

3.2.1.4 Sulfidation of Metal(s) Supported on Pillared Clay Catalysts

The sulfidation of the metal-supported, chromia-pillared Wyodak and metal-supported Wyodak was carried out by placing the desired coal sample in a 75-mL tubing bomb. The tubing bomb was pressurized with a 100-psig mixture of hydrogen sulfide and hydrogen (9:1 v/v). The bomb was lowered into a fluidized-bed sand bath heated to 200°C. The bomb was heated at this temperature for 2 hours, degassed, and heating was continued for 12 hours.

3.2.1.5 Elemental Analysis

Total sulfur determination was done with a LECO model 532 sulfur analyzer, using the ASTM D1551 method. The method of Vogel (2) was used for chlorine analysis. Carbon, hydrogen, and nitrogen analyses were performed on a Control Equipment Corporation Model 240XA Elemental Analyzer.

Proton and ^{13}C NMR spectra were obtained in dichloromethane-d_2 with TMS standard on a Varian XL200 NMR spectrometer. Infrared spectra were obtained in KBr on either a Perkin Elmer Model 283 spectrometer or a Nicolet 20SXB FTIR spectrometer equipped with a mercury cadmium telluride (MCTA) detector and a Nicolet 1280 computer with a fast Fourier transform coprocessor.

Quantitative GC/FID analyses were performed with a Hewlett Packard 5880A gas chromatograph equipped with a J&W 60 m x 0.25 mm (ID), 1.0 micron DB-1701 capillary column. n-Octadecane was the internal standard. Isotope dilution GC/MS was performed on a Finnigan 800 ITD ion trap detector with an HP 5890A gas chromatograph and a J&W 30 m x 0.32 mm (ID), 1.0 micron film of DB-5. Phenol, naphthalene, and tetralin were determined with per-deutrated analogs as the respective internal standards. A 15 m x 0.25 mm (ID), 0.25-micron DB-5 film capillary column was used for the analysis of high boiling components.

3.2.2 Characterization of Solid Acid Catalysts: Acidity Measurements

The acidity of the solid acid catalyst, zinc chloride supported on silica, was further determined by pyridine adsorption and desorption methods using FTIR and thermogravimetric (TGA) methods.

3.2.2.1 Infrared Method

A small amount of sample (100 mg) was placed in a glass chamber attached to a vacuum pump, a gas inlet, and a gas outlet. The chamber was evacuated, and argon saturated with pyridine was introduced into the chamber until the weight increase ceased. At this stage the chamber was evacuated until the physisorbed pyridine was removed as indicated by the constant weight of the base absorbed sample. The infrared spectra of the pyridine-absorbed catalyst was obtained on the Nicolet FTIR spectrometer with the diffuse reflectance cell. Infrared spectral data are presented in Table 1.

TABLE 1

INFRARED ABSORBANCE OF PYRIDINE-ADSORBED CATALYST

Band	Absorbance	Extinction Coefficient (3)
1440 cm^{-1} (Lewis-Pyridine Band)	0.47	0.084
1536 cm^{-1} (Brönsted-Pyridine Band)	0.094	0.058
Lewis/Brönsted Sites = 3.4		

3.2.2.2 Thermogravimetric Method

Total acidity of the catalyst was determined from the chemisorption of pyridine on the catalyst surface using a thermogravimetric analysis (TGA) technique.

Approximately 20 mg of catalyst were placed on the sample pan of the DuPont 951 thermogravimetric balance module, which was interfaced with a DuPont 1090 Thermoanalyzer (controller and data station). The sample was purged at ambient temperature with argon until constant weight was achieved (several minutes). The argon flow was then stopped, and the sample chamber was evacuated. The vacuum pump continued to hold the partial vacuum until constant weight was once again achieved. The pump was then turned off, and a flow of pyridine-saturated argon at ambient temperature was introduced into the sample chamber. The pyridine-argon flow continued for 180 minutes, at which time the weight gained by the sample had nearly ceased. The chamber was again evacuated, still at ambient temperature, and held under partial vacuum for 40 minutes. When constant weight was achieved, the temperature was increased at 20°C/min to 105°C, where it was held for 30 minutes. The temperature was then increased by 2°C/min to 202°C and held there for 30 minutes, followed by a temperature increase of 20°C/min to 300°C where it was held for 60 minutes. Upon reaching constant weight, the experiment was terminated. The 1090 Thermoanalyzer records time, temperature, and weight during experimentation (Figure 1). On reducing the data, dw/dt is calculated and the data are reported on a plot of wt% and dw/dt versus time and wt% and dw/dt versus temperature.

3.3 Results and Discussion

3.3.1 Characterization of Catalysts

Mixtures of silica gel with zinc sulfate, and tin(II) chloride were characterized by elemental analysis, infrared spectroscopy, and thermogravimetric methods.

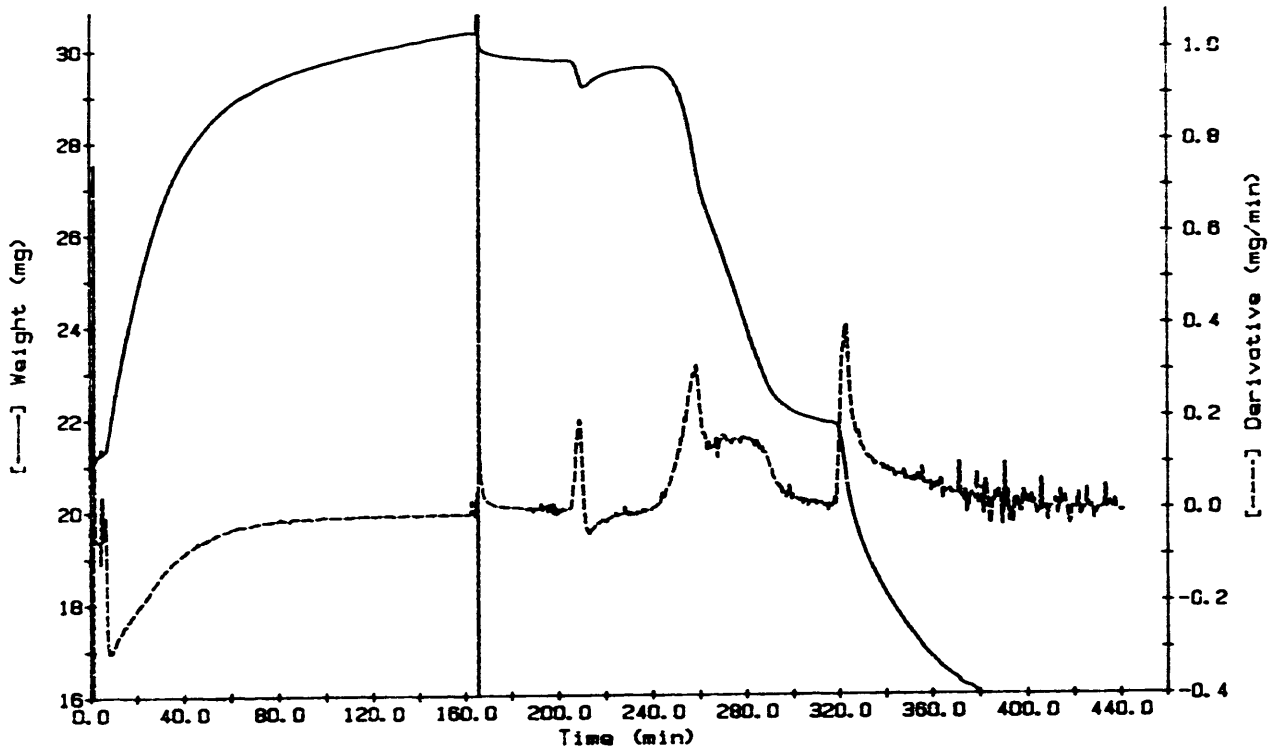

Figure 1. Thermogravimetric analysis: pyridine absorption/desorbtion.

3.3.1.1 Elemental Analyses

Elemental analyses of the tin(II) chloride and zinc sulfate mixtures with silica gel indicated that no loss of chloride and sulfate occurred during the heating procedure. Most of the salt (99%) is present, and only a small amount of chlorine or sulfate is present as Si-O-SnCl or (Si-O-Zn)HSO_4. In the silica gel zinc chloride (SZC) catalyst, 2% of chlorine is present as Si-O-ZnCl. The catalyst is a mixture of zinc chloride, zinc chloride complexed with silica gel, and oxyzinc salt.

3.3.1.2 Infrared Method

Infrared spectroscopy of the pyridine complex was used to determine the relative proportion of Lewis and Brönsted acid sites in the silica gel zinc chloride catalyst. In the infrared spectrum of the pyridine-absorbed silica gel zinc chloride catalyst, the bands at 1440 and 1536 cm^{-1} are assigned to pyridine-Lewis acid coordination bond, and pyridine-Brönsted acid bond, respectively. The relative intensities of these bands were converted to the concentration ratio by using the respective extinction coefficients. The ratio of the concentration of Lewis sites to Brönsted sites was 3.4 (Table 1).

3.3.1.3 Thermogravimetric Analysis

The thermogravimetric technique was used to determine the total acid sites and stability of the catalyst. In the TGA experiment, the weight of the catalyst increased from 21 mg to 29.74 mg, upon pyridine absorption followed by evacuation at ambient temperature. The weight increase is due to the chemical adsorption of the pyridine at both Lewis and Brönsted acid sites and,

therefore, is a measure of the total acidity of the catalyst. Upon slowly heating the catalyst (2°C/min.) to 300°C, all of the chemically adsorbed pyridine could be removed. In the temperature range of 105°-140°C, 2.9 mg of pyridine was lost, and the rest (5.8 mg) was lost in the range 140°-202°C. The inflection in the curve at 140 is believed to represent the onset of pyridine loss from the Brönsted acid sites, but the loss of pyridine from the Lewis acid sites continued to occur as the temperature was raised. Thus the relative amounts of Lewis and Brönsted sites could not be obtained from these data, only the total amount of acid sites (5.04 mmoles/g catalyst). Heating above 300°C resulted in the loss of chlorine due to decomposition and or sublimation of zinc chloride from the catalyst surface. In the solid state the catalyst is only stabile up to 300°C.

3.3.2 Catalytic Testing

3.3.2.1 Catalytic Hydrotreating of 1-Methylnaphthalene

1- and 2-methylnaphthalenes were used to investigate the relative kinetics of the hydrotreatment reactions of polynuclear aromatics with solid acid catalysts (silica gel zinc chloride). The reactions were carried out by heating 1- or 2-methylnaphthalene and silica gel zinc chloride in the presence of 1000 psig of molecular hydrogen at 300°C for reaction times ranging from 5 minutes to 24 hours. The effect of reaction time in the hydrotreating was investigated.

In a typical run, 1.0 g of 1- or 2-methylnaphthalene and 0.5 g of silica gel zinc chloride were placed in a tubing bomb (12-mL microreactor). The microreactor was evacuated, pressurized with 1000 psig of hydrogen, and placed in a rocking autoclave heated to 300°C. At the end of the reaction period, the microreactor was cooled to room temperature, degassed, and opened. The desired amount of the internal standard was added to the product slurry, and the product slurry was transferred into a centrifugation tube by washing with methylene chloride. The solid catalyst was removed by centrifugation. The liquid sample was analyzed by GC/FID and GC/FTIR/MS.

The chlorine analysis of the recovered catalyst did not indicate any loss of chlorine during reaction. Detailed characterization of the recovered catalyst to determine the possible loss of catalytic activity is in progress.

The reactions of 1- and 2-methylnaphthalenes with silica gel zinc chloride catalyst under different conditions gave the products indicated in Table 2. These products indicated that three reactions--namely, isomerization (rearrangement), hydrogenation, and demethylation (hydrocracking)--occurred during the catalytic hydrotreating of 1-methylnaphthalene. The formation of polymethylnaphthalenes is regarded as being a major part of the demethylation reaction (transmethylation).

The reaction of 1-methylnaphthalene with silica gel zinc chloride at 300°C and in the presence of 1000 psig of hydrogen for 5 minutes gave 1- and 2-methylnaphthalenes in the ratio of 5.14. Methyltetralins were the minor products from this reaction (6% yield). A 1-hour reaction time gave a ratio of 0.8, and a 24-hour reaction time gave 0.07. Under these conditions, almost 89% of the starting material was converted into products. Major products were tetralin, methyltetralins, naphthalene, and 1- and 2-methylnaphthalenes. Minor products were benzene, toluene, and decalin. Small amounts of

TABLE 2

REACTIONS OF METHYLNAPHTHALENES
(Reaction Temp. = 300°C, 1- or 2-Methylnaphthalene = 1.0 g, H_2 = 1000 psig, Subst./Catalyst = 0.5, Catalyst = Silica Gel Zinc Chloride (SZC))

Subst.	Time (hr)	Conv. (%)	1-Menaph./2-Menaph. Ratio	Major Products
1-Menaph*	0.08	6	5.15	Methyltetralins
1-Menaph	1	6	0.8	Methyltetralins
1-Menaph	24	89	0.07	Naphthalene Tetralin Methyltetralins
2-Menaph	1	15	0.36	Naphthalene Tetralin Methyltetralins Benzene Toluene Indan
2-Menaph	3	32	0.42	Naphthalene Tetralin Decalin Benzene Alkylbenzenes
2-Menaph	24	89	0.09	Naphthalene Tetralin Methyltetralins

* Methylnaphthalene

cyclohexane, methylcyclohexane, ethylbenzene, o-xylenes, indan, and C_3-C_5 were also identified in the product. In order to determine whether the reaction actually achieves an equilibrium with respect to 1- and 2-methylnaphthalene, the reaction of 2-methylnaphthalene was also investigated. The reaction of 2-methylnaphthalene at 300°C for 1 hour and in the presence of 1000 psig of hydrogen gave 1- and 2-methylnaphthalene (85% of the starting material), and the ratio of 1- and 2-methylnaphthalenes was 0.36. Small amounts of benzene, toluene, indan, naphthalene, and methyltetralins were also produced during reaction. When the same reaction was carried out for 3 hours, 68% of the substrate was recovered as a mixture of 1- and 2-methylnaphthalenes in the ratio of 0.423. The remainder of the starting material was converted into products. Major products from this reaction were benzene, toluene, o-xylenes, ethylbenzene, decalin, naphthalene, and tetralins. Upon heating 2-methylenaphthalene and 1000 psig of hydrogen with silica gel zinc chloride for 24 hours, almost 89% of the substrate was converted into products other than methylnaphthalenes. 1- and 2-methylnaphthalenes constituted about 11% of the products in the ratio of 0.09. Product distribution was the same as that obtained in the reaction of 1-methylnaphthalene under the same conditions.

The data from the two sets of reactions at 300°C indicate that the isomerization reaction is rapid at this temperature. It apparently does not reach an exact equilibrium point, owing to different reactivities of the 1- and 2-methylnaphthalenes in the subsequent reactions (hydrogenation, hydrocracking) that occur at slower rates. This lack of steady-state concentrations makes kinetic analysis difficult. We may conclude that the isomerization reaction of 1- and 2-methylnaphthalene proceeds to an approximate equilibrium ratio (1-/2-) of 0.4 in a time of 1 hour at this temperature. Over longer periods (1 day), the ratio decreases to less than 0.1. Extensive conversion to the methyltetralin mixtures and naphthalene occurs over the extended period.

In the initial stages of the reaction, isomerization predominates as indicated by the 5-minute and 1-hour reactions. As the reaction time increases, the isomer mixture is converted into naphthalene via demethylation, and to methyltetralins via hydrogenation of either of the rings of the methylnaphthalene substrates. The demethylation is accompanied by formation of di- and trimethylnaphthalenes. Extensive hydrocracking of the tetralins resulted in a mixture of alkylbenzenes. Small amounts of cyclohexane, methylcyclohexane, decalin, and indans were formed in addition to the above products. The major reaction sequences involving the methylnaphthalenes are presented in Figure 2.

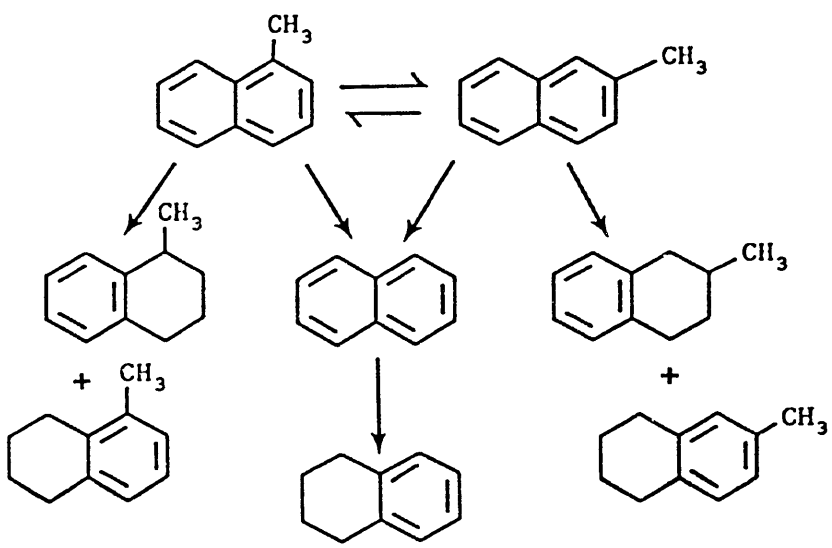

Figure 2. Hydrogenation/hydrocracking/isomerization of methylnaphthalenes.

3.3.2.2 Catalytic Hydrotreating of Cis-Decalin

The reactions of cis-decalin were carried out at 400°C for 1 hour. The reaction variables were hydrogen, catalyst, solvent, and additive (bibenzyl). The reaction conditions and conversion data are given in Table 3. The reactions were carried out in a microreactor. The reaction procedure was the

same as described for the reactions of methylnaphthalenes. The product slurry was mixed with the appropriate internal standard and extracted with methylene chloride. The solid was separated by centrifugation. The methylene chloride soluble fraction was analyzed by GC/FID and GC/FTIR/MS. The solid residue (methylene chloride soluble fraction) was weighed and analyzed by elemental analysis and infrared spectroscopy. The methylene chloride insoluble fraction was mainly recovered catalyst.

TABLE 3

CIS/TRANS CONVERSION DATA FOR REACTIONS OF CIS-DECALIN
(Reaction Temp. = 400°C, Time = 1 hr)

	Amounts of Reactants (g)				
Catalyst	Cis-Decalin	Bibenzyl	Solvent	Hydrogen (psig)	Cis/Trans Conversion (%)
None	1.00	0	None	1000	1
SZC* 0.5	1.00	0	None	1000	17.4
SZC 0.03	0.07	0	Hexadecane 2.00	1000	18.4
SZC 0.05	0.10	0.10	Hexadecane 2.00	1000	13.1
SZC 0.05	1.00	0.10	None	0	18

*SZC = Silica gel zinc chloride

Upon heating at 400°C for 1 hour in the presence of 1000 psig of hydrogen, only 1% of cis-decalin was converted into trans-decalin. However, when the same reaction was carried out by heating 1.0 g of cis-decalin with 0.5 g of silica gel zinc chloride and 1000 psig of hydrogen under the same conditions, 17.4% of trans-decalin was formed. In the reaction of 0.07 g of cis-decalin in 2.0 g of hexadecane with 0.03 g of silica gel zinc chloride in the presence of 1000 psig of hydrogen at 400°C for 1 hour the conversion of cis-decalin was 18.4%. The reaction of a solution of cis-decalin and bibenzyl (0.1 g each) in 2.0 g of hexadecane with 0.05 g of silica gel zinc chloride and 1000 psig of hydrogen at 400°C for 1 hour resulted in slightly less conversion (13.1%). When the reaction of cis-decalin (1.0 g) containing 0.10 g bibenzyl was carried out with silica gel zinc chloride at 400°C for 1 hour and in the absence of hydrogen, the conversion of cis-decalin was 18%, which is essentially the same as that observed for the reaction of cis-decalin in the presence of hydrogen and absence of bibenzyl. Almost quantitative amounts of bibenzyl and decalins were recovered at the end of the reaction.

The results are consistent with an acid-catalyzed isomerization mechanism. The very small amount of reaction in the absence of catalyst indicates that free radical reactions are not important in this system at this temperature. The catalyst (Lewis acid site) can abstract a hydride ion from the decalin to give a tertiary carbonium ion. The carbonium ion intermediate then is converted back to cis- and trans-decalin by regaining the hydride ion. The equilibrium concentration ratio for cis/trans decalin is about 0.2. The conversions obtained with this system indicate that the reaction has not progressed very far toward the equilibrium position. The most important finding is that the addition of bibenzyl does not result in any increase in the cis to trans conversion. This lack of interaction means that the carbonium ion intermediates produced in the reaction of the bibenzyl with the catalyst do not abstract hydride ions from the tertiary carbons of the cis-decalin.

3.3.2.3 Catalytic Hydrotreating of Model Compounds

The reactions of model compounds such as bibenzyl, diphenylpropane, and neopentylbenzene were carried out with solid acid catalysts such as silica gel zinc chloride, silica gel zinc sulfate, and silica gel tin(II) chloride. The reactions were carried out at 350°C for 3 hours both with and without hydrogen. These reactions were carried out in the manner described for the reactions of methylnaphthalenes. At the end of the reaction, the microreactor was cooled in dry ice/acetone slurry, degassed, and opened. The product slurry from the reaction was mixed with the appropriate internal standard, transferred into a centrifugation tube with methylene chloride, and the solid catalyst was separated by centrifugation. The liquid product was analyzed by GC/FID and GC/FTIR/MS analyses. The solid product was washed with methylene chloride, vacuum dried, and weighed. The elemental analysis of the methylene chloride insoluble product indicated this product to be essentially the recovered catalyst.

Reactions of bibenzyl with silica gel tin(II) chloride and silica gel zinc sulfate indicated a very small conversion of bibenzyl into products. Traces of benzene and toluene were the only products from these reactions. The elemental analysis of the methylene chloride insoluble fractions indicated these products to be the same as the original catalyst.

The effect of hydrogen on the conversion of bibenzyl and the product distribution was investigated by carrying out reactions both in the presence and the absence of hydrogen. The percent conversion measured as the disappearance of the substrate was almost the same in both these reactions. However, the product distribution was significantly affected by the presence of hydrogen (Table 4). The reaction with no hydrogen produced 7% of coke which is formed due to retrograde condensation reactions. Also, the amount of condensation products (substituted bibenzyls) increased from 18% to 27% in the absence of hydrogen. In the presence of hydrogen, the amount of benzene was only slightly higher, but the amount of ethylbenzene increased considerably. It is believed that the reaction of bibenzyl involves ipso protonation followed by the cleavage of an aryl-methylene bond, leading to the formation of benzene and the phenylethyl carbonium ion. The phenylethyl carbonium ion can undergo a variety of reactions (Figure 3) to give products. The overall mechanism of the acid-catalyzed hydrocracking of bibenzyl is depicted in Figure 4. The fact that ethylbenzene forms even in the absence of molecular hydrogen indicates that hydride transfer from Scholl intermediates or

TABLE 4

CATALYTIC HYDROCRACKING OF BIBENZYL
(350°C, 3 hrs, 5.49 mmols bibenzyl, 0.5G SZC catalyst)

Reductant Amount	Conversion (%)	Major Products (mmols)	
None	83	Benzene	(3.2)
		Toluene	(0.2)
		Ethylbenzene	(0.8)
		Cond. Prod.	27%
		Coke	7%
Hydrogen 1000 psi	80	Benzene	(3.54)
		Toluene	(1.35)
		Ethylbenzene	(0.15)
		Cond. Prod.	18%
		Coke	0%

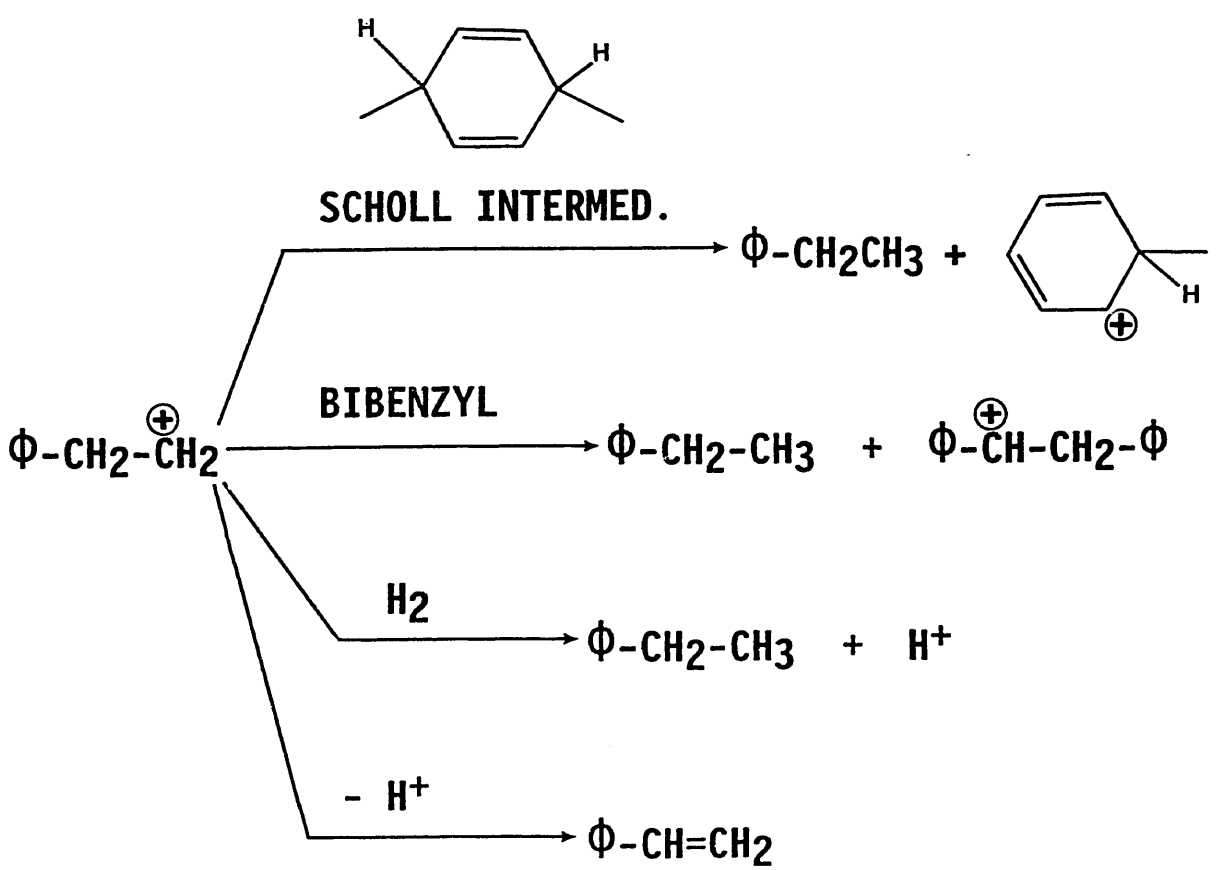

Figure 3. Reactions of phenylethyl carbonium ion.

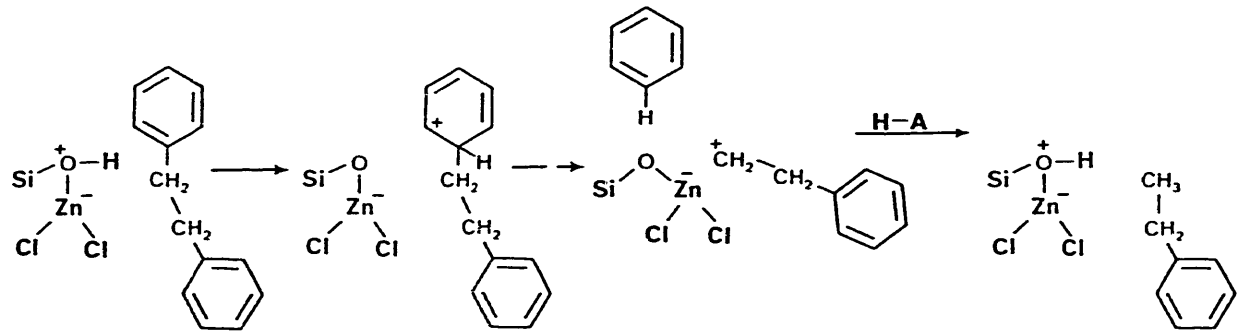

Figure 4. Mechanism for hydrodealkylation of bibenzyl.

hydroaromatic condensation products is the major mechanism for formation of ethylbenzene. Hydrogen may be indirectly involved through reductions of these condensation products.

Diphenylpropane and neopentylbenzene were used to investigate the catalysis mechanism of silica gel zinc chloride. The reactions were carried out at 350°C for 3 hours in the presence of 1000 psig of hydrogen. The reaction procedure and product work-up have been described earlier. The product slurry was separated into methylene chloride soluble and insoluble fractions. The methylene chloride soluble fraction was mixed with the appropriate internal standard and analyzed by quantitative GC using a petrocol column. The methylene chloride insoluble fraction was analyzed by elemental analysis and was found to be essentially the recovered catalyst. The product distribution and the percent conversion for these reactions are presented in Table 5.

Diphenylpropane gave benzene and indan as the major products. The formation of benzene may be due to the ipso protonation of the aromatic ring followed by aryl-methylene bond cleavage. The phenylpropyl carbonium ion then undergoes rearrangement in the presence of the acid catalyst to give indan as the second major product. The minor products from this reaction were C_1-C_2 benzenes. Possible mechanisms leading to the formation of these products are shown in Figures 5 and 6.

The conversion of neopentylbenzene was much smaller than that of diphenylpropane, and a variety of products was obtained. The major product from this reaction was benzene, which is formed due to the ipso protonation of the aromatic ring followed by aryl-methylene bond cleavage. The neopentyl carbonium ion rearranges to produce 2-methylbutane (Figure 7). Toluene and 2-methylpropane may have been formed from the Lewis acid catalyzed cracking of neopentylbenzene (Figures 8 and 9).

4.0 REFERENCES

1. Olson, E.S. "Quarterly Technical Progress Report for the Period July to September 1989," UND Energy & Environmental Research Center.

2. Bassett, J., et al. Vogel's Textbook of Quantitative Inorganic Analysis; 4th ed., Longman Scientific & Technical: London, 1978, pp 301-304.

3. Datka, J.; Tuznik, E. J. Catal. 1986, 102, 43-51.

TABLE 5

CATALYTIC HYDROCRACKING OF DIPHENYLPROPANE AND NEOPENTYLBENZENE
(350°C, 3 hrs, Subst./Cat. = 2, H_2 = 1000 psig)

Catalyst (g)	Substrate (mmols)	Conversion	Major Products (mmols)	
SZC	DPP	76	Indan	(1.39)
0.25	(2.6)		Propylbenzene	(0.08)
			Ethylbenzene	(0.06)
			Toluene	(0.05)
			Benzene	(2.43)
			Cond. Prod.	0%
			Coke	0%
SZC	NPB	26	Benzene	(0.29)
0.25	(3.5)		2-Methylbutane	(0.08)
			2,2-Dimethylpropane	(0.003)
			Toluene	(0.06)
			2-Methylpropane	(0.04)
			Butane	(0.003)
			Pentane	(0.001)
			Ethylbenzene	(0.03)

SZC = Silica gel zinc chloride
DPP = Diphenylpropane
NPB = Neopentylbenzene

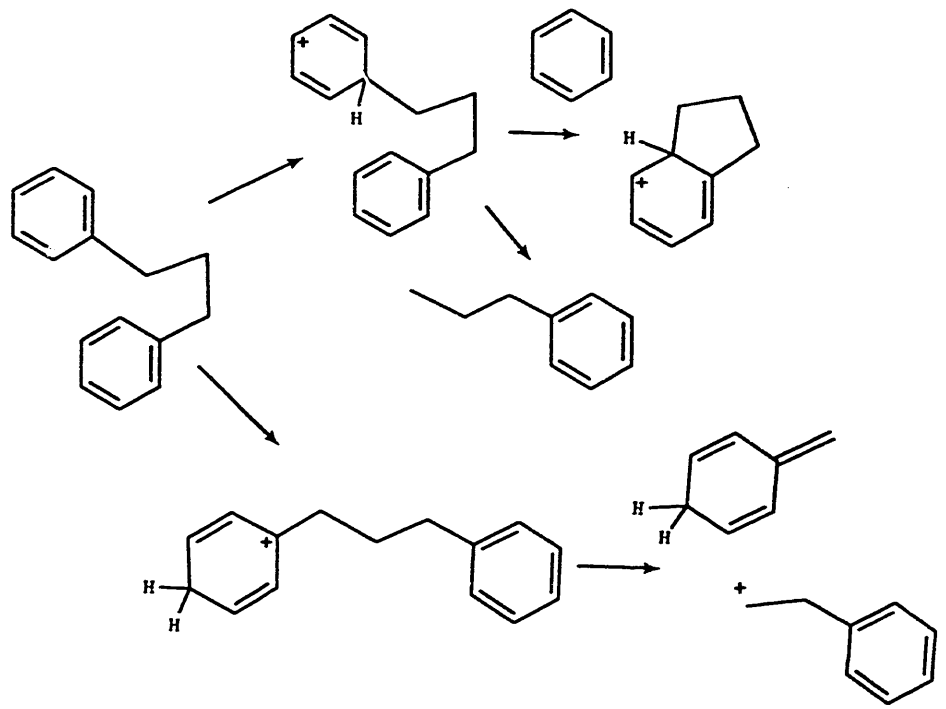

Figure 5. Mechanism for hydrodealkylation of diphenylpropane (Brönsted Site).

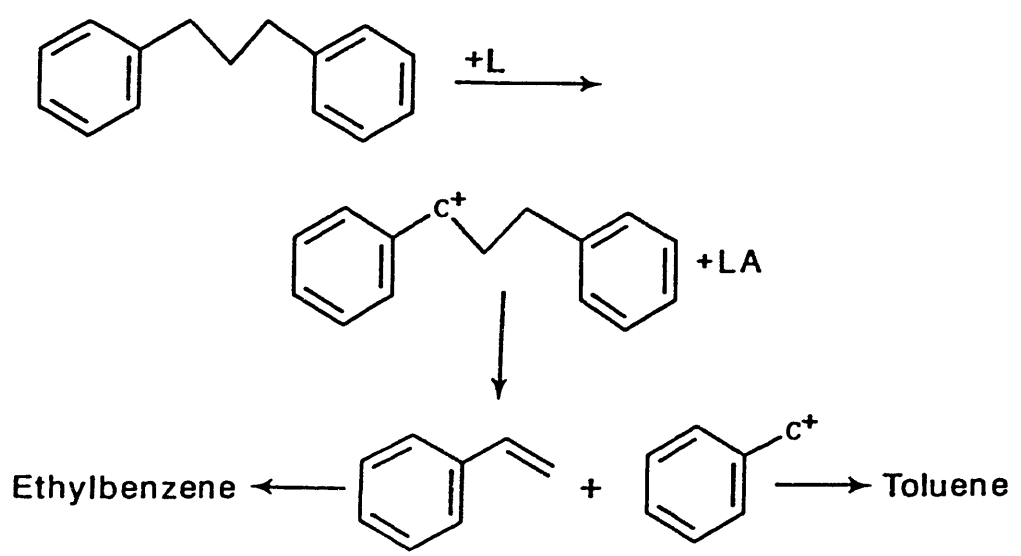

Figure 6. Mechanism for hydrodealkylation of diphenylpropane (Lewis Site).

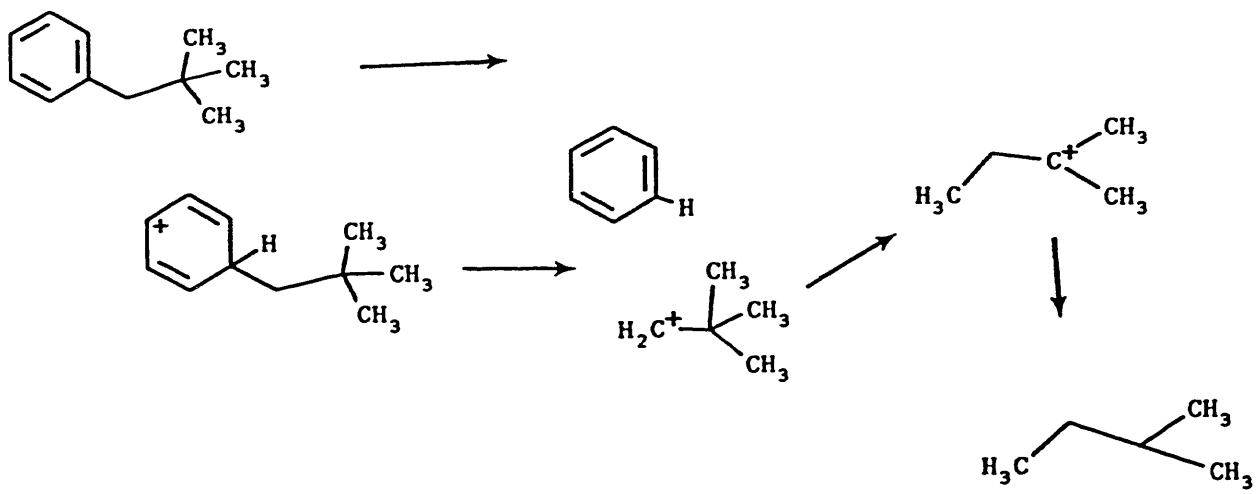

Figure 7. Mechanism for hydrodealkylation of neopentane (Brönsted site--ipso cleavage).

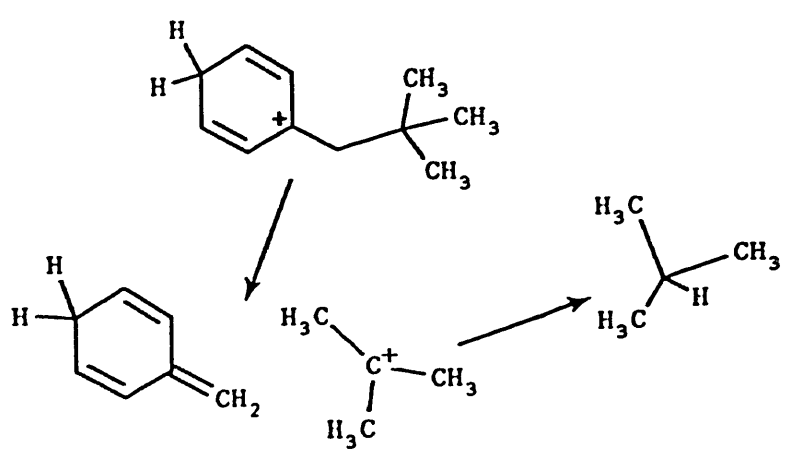

Figure 8. Mechanism for hydrodealkylation of neopentane (Brönsted site--alpha cleavage).

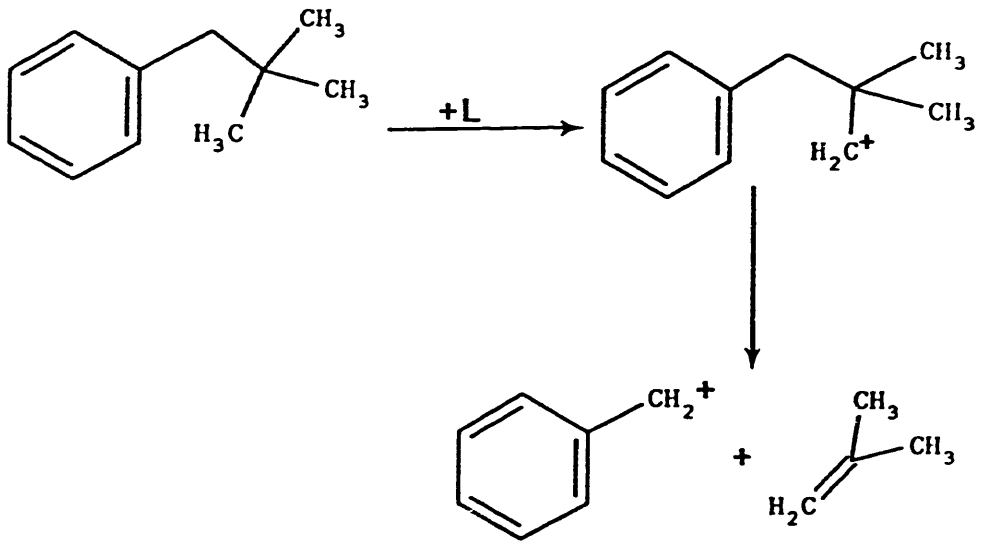

Figure 9. Mechanism for hydrodealkylation of neopentane (Lewis site--alpha cleavage).

3.5 Gasification Ash and Slag Characterization

GASIFICATION ASH AND SLAG CHARACTERIZATION

Quarterly Technical Progress Report
for the Period of January - March 1990

by

Steven A. Benson, Jan W. Nowok, and Sumitra R. Ness
Energy and Environmental Research Center
University of North Dakota
PO Box 8213, University Station
Grand Forks, ND 58202

Contracting Officer's Technical Representative: H. Fred Bauer

for

U.S. Department of Energy
Morgantown Energy Technology Center
3610 Collin Ferry Road
Morgantown, West Virginia 26505

May 1990

Work Performed Under Cooperative Agreement No. DE-FC21-86MC10637

TABLE OF CONTENTS

LIST OF FIGURES

LIST OF TABLES

GASIFICATION ASH AND SLAG CHARACTERIZATION

1.0 EXECUTIVE SUMMARY

This report summarizes the accomplishments for the period of January through March 1990.

Task A: Construction of the pressurized drop-tube furnace system that will be used to simulate gasification conditions has been completed, and operation will begin when the necessary permits have been approved.

Task B: The computer code PHOEBE was tested against the Al_2O_3-SiO_2 binary phase diagram. A typographical error in the data base was discovered and eliminated. Graphical results will be presented in following monthly reports.

Task C: Determination of physiochemical effects present during interfacial surface tension measurements were studied.

1) Effect of Time: The data shows that there is an increase in the interfacial surface tension in the first 30 minutes of measurement, the time required to achieve uniform, steady-state conditions in the molten slag droplet.

2) Effect of Atmosphere: The data show that measurements conducted in a CO/CO_2 atmosphere are less than those conducted in an H_2/N_2 atmosphere.

3) Effect of Temperature: The data show significant changes for temperatures below the temperature of critical viscosity, T_{cr}, and no significant changes for temperatures above T_{cr}. This effect is attributed to the presence of surface active phases and polymerization of silicates in the slags. Please refer to the Results and Discussion section of this report for further information.

2.0 OBJECTIVES

2.1 Task A: Inorganic Reactions

This task involves determining the reactions and interactions that coal inorganic constituents undergo during gasification processes. Two coals: Sufco, a Utah bituminous coal, and Jacob's Ranch, a Wyoming subbituminous coal, will be studied. The chemical and mineralogical transformations will be studied under simulated gasification conditions using a modified version of the pressurized drop-tube furnace system at the EERC. The coals will be characterized using chemical fractionation, computer-controlled scanning electron microscopy (CCSEM), and scanning electron microscopy point count (SEMPC). SEMPC data can be used to determine the viscosity and relative reactivity of the liquid phases as well as the bulk chemical composition of the sample. This data will show both the partitioning of the ash species as

well as the effect of char formation on the ash species with respect to potential sintering behavior.

2.2 Task B: Partitioning of Ash Components

The relative quantity and composition of the amorphous phases on char and ash particles provide an indication of the deposition propensity of coal ash under gasification conditions. The reactivity between individual char and ash particles is also determined by the nature of the amorphous phase. The reactivity propensity is based on the base-to-acid ratios of individual ash components. Understanding the role of the amorphous phase will aid in the understanding of partitioning and deposition phenomena. The data may also be used to develop a scale, index, or empirical equation to measure the degree of reactivity between amorphous phases. Task B will involve the detailed comparison of the ash species formed in the pressurized drop-tube furnace system with the parent coal. The gas-entrained species will be determined by on-line sampling in the furnace. Work will also continue in the development of a vapor-liquid-solid thermochemical equilibrium code. Data from this code will be used to theoretically predict ash partitioning.

2.3 Task C: Ash Sintering Under Gasification Conditions

Sintering is an ash characteristic that can be used to predict ash behavior. The behavior of mineral matter in coal gasification is different than that in the combustion systems and is generally characterized by lower temperatures, more reducing conditions, and longer residence times. The goal of Task C is to study sintering mechanisms in coal ash systems to determine the effects of various additives on sintering phenomena.

2.4 Associated Task

As this project involves development of methodologies to predict ash behavior in gasification systems, we plan to enhance our relationship with industrial-scale operators such as DOW, Shell, and Texaco. This will ensure that our approach to studying ash behavior in gasification systems can be validated as they are developed.

3.0 RESULTS AND DISCUSSION

3.1 Physiochemical Effects Determining the Accuracy of Interfacial Surface Tension Measurement of Coal Ashes

The sessile drop technique has been used to determine the interfacial surface tension of Beulah Blend, Illinois #6, and Pittsburgh #8 coal ashes in various atmospheres. The following is a discussion of the physiochemical effects determining the accuracy of the measurement. The data shows that the interfacial surface tension measured below the temperature of critical viscosity, T_{cr}, are lower than those determined above T_{cr}. This effect is attributed to the nonequilibrium state of the liquid-vapor surface tension, η_{LV}. The difference in the chemical composition of the molten drop surface

and the bulk chemical composition of the drop creates a nonequilibrium state. The difference in chemical composition between the surface and bulk can be attributed to evaporation of sodium, the random distribution of surface active phases such as silca-rich clusters, and the polymerization of silicate structures in the slag. Interfacial surface tensions measurements did not vary significantly with temperature above T_{cr}.

Ordinarily, surface tension is an intensive thermodynamic property that should be measured on the systems that are free from extraneous mechanical, electrical or chemical interactions. Surface tension measured in the presence of an interacting gas is termed interfacial surface tension. The calculation of surface tension employs procedures which permit fitting of measured drop profile to a theoretical profile by varying two parameters, ß and b, using a nonlinear regression program. The shape factor, ß, and the radius curvature, b, at the drop apex are related by the equation:

$$\beta = \frac{b^2 * g}{\gamma} * (d_m - d_{gas}) \qquad [1]$$

where η is the surface tension, g is the gravitational acceleration which depends on the drop size, and d_m and d_{gas} are the densities of liquid slag and gas, respectively. Two principle errors based on the measurement of the drop profile and density were discussed in the article (1). The purpose of this task is to determine all possible physiochemical effects that influence the accuracy of interfacial surface tension and viscosity measurements of coal ash slags under reducing atmospheres corresponding to gasification conditions.

3.2 Experimental

Beulah lignite, Pittsburgh #8, and Illinois #6 coals were pulverized to -60 mesh and ashed in air at 800°C for 24 hours. The resulting ashes were slagged at 1500°C and kept in a homogeneous state by rotating the viscometer bob. Controlled atmospheres of air, 8%H_2-92%N_2, and 60%CO-40%CO_2 were used in the interfacial surface tension and viscosity measurements. The samples used in the measurements were first slagged, quenched in air at room temperature, and finally ground to -38 mesh. This procedure produced a homogeneous sample with a uniform distribution of all coal ash components. Therefore, errors in the determination of interfacial surface tension due to a nonequilibrium state caused by a nonuniform distribution are theoretically avoided. Homogenation of samples increases the required sample preparation time. Thus the evaporation of light elements such as sodium from the surface of a sessile drop over a long duration may occur, affecting the measured values of interfacial surface tension. During evaporation, the chemical potential of surface atoms is varied from those in the bulk. As a consequence of that, the interfacial surface tension also changes.

Two kind of pellets were used: pulverized glassy slag and small pieces of the crashed slag. The pulverized glassy coal ash was pressed by hand into

a pellet with diameter about 1 cm, centered on a plane surface of vitreous carbon, and placed in the horizontal tube furnace preheated to 900°C. Previous work showed that for drops with diameters greater than 2 cm, the surface tension of mercury increased progressively with drop diameter and decreases slightly with diameters less than 1 cm (2). For the work conducted in the Gasification Ash and Slag project, the sessile drops were exposed to various mixtures of gases, air, H_2/N_2 (8/92), and CO/CO_2 (60/40). A continuous flow of gas (60 cc/min) was maintained throughout the experiment. The profile of a sessile drop was photographed at designated temperatures and times.

The coordinates of sessile drop were measured both directly from the film using an optical microscope and from the image projected onto graph paper. Calculation of the surface tension was performed by a computerized nonlinear curve-fitting procedure. Chemical compositions of coal ashes were determined after surface tension measurements by x-ray fluorescence analysis. The compositions of the ashes on a sulfur-free basis are listed in Table 1.

Raask (3) has suggested that in iron-rich slags, iron carbide might be formed at the slag-vitrous carbon interface, causing carbon monoxide evolution above 1400°C. The reaction between iron oxide bearing slags and solid carbon was significant in $FeO-SiO_2$ slags. Lime-containing slags were found to react more slowly with carbon (4). These important side reactions created difficulties in the interpretation of the experimental work.

During the Gasification Ash and Slag work, the process of gas generation inside the slag droplet caused changes in the sessile drop shape. This effect was determined by the calculation of slag density from the sessile drop coordinates. A number of experiments have shown a significant change of density for slag droplets exposed to air at temperatures above 1350°C. To study this effect, interfacial surface tension measurements determined below 1350°C were made after the sample had been held at constant temperature for at least 30 min. It should be pointed out that the temperature of sessile drop formation is a characteristic one and occurs below 1350°C for most coal ashes. Thus the temperature of sessile drop formation was selected as a reference temperature. For homogenated slags in CO/CO_2, the interfacial surface tension measured above 1400°C did not show a significant change in slag droplet density. Table 2 illustrates examples of density variation as the function of temperature for several slags exposed to CO/CO_2 atmosphere. All results of interfacial surface tension with density error larger than 5% were rejected.

Viscosity was measured using a rotating bob viscometer in CO/CO_2 (60/40) atmosphere to determine the temperature of critical viscosity. Measurements were started at the highest temperature and stepped down to lower temperatures until the upper limit of the viscometer was approached.

Table 3 lists some of the interfacial surface tension data for Illinois #6 slags prepared in CO/CO_2 atmosphere (Runs No. 13-15), which were held at temperatures for complete spherical formation in CO/CO_2 for 0-40 min. The data shows evidence that there is an increase of interfacial surface tension within 30 min, likely due to the stabilization of η_{LV}. This amount of time is required to achieve steady-state conditions in the molten slag.

TABLE 1

COMPOSITION OF COAL ASHES (WEIGHT PERCENT EXPRESSED AS EQUIVALENT OXIDE) USED IN THE INTERFACIAL SURFACE MEASUREMENTS

Run No.	Coal Ash	SiO_2	Al_2O_3	Fe_2O_3	TiO_2	CaO	MgO	Na_2O	K_2O
	A. Prepared in air								
1	Beulah	37.5	15.1	11.3	1.6	21.6	6.1	5.7	0.8
2	Pittsburgh #8	50.9	20.2	19.1	1.2	4.7	1.1	0.0	2.6
3	Illinois #6	46.7	20.7	21.1	1.3	6.4	1.1.	0.0	2.7
	B. Prepared in H2/N2 (8/92)								
4	Beulah	37.9	15.3	11.1	1.6	22.2	5.5	5.7	0.7
5	Pittsburgh #8	51.2	20.7	18.0	1.2	4.8	1.2	0.0	2.6
6	Illinois #6	47.7	19.6	20.7	1.3	6.5	1.2	0.0	2.8
	C. Prepared in CO/CO_2 (60/40)								
7	Beulah	38.0	15.3	10.9	1.6	22.4	5.1	5.8	0.7
8	Beulah + Limest.	33.1	23.0	10.1	1.3	26.1	2.9	2.8	0.7
9	Beulah + Dolom.	34.2	16.2	9.7	1.5	25.8	8.0	4.2	0.5
10	Pittsburgh #8	51.1	20.6	18.2	1.2	4.9	1.2	0.0	2.6
11	Pitt. + Limest.	43.1	20.7	16.2	1.1	16.0	0.8	0.0	2.2
12	Pitt. + Dolom.	45.9	20.3	16.6	1.1	10.1	3.6	0.0	2.2
13	Illinois #6	47.9	19.5	20.6	1.3	6.7	1.2	0.0	2.8
14	Ill. + Limest.	40.9	18.6	18.9	1.1	17.5	0.7	0.0	2.3
15	Ill. + Dolom.	42.4	20.2	18.0	1.1	12.4	3.5	0.0	2.3

TABLE 2

DENSITY OF SLAG DROPLETS CALCULATED FROM THE SESSILE DROP

	Density, g/cm(3)		
Temperature °C	Beulah Run No.7	Pittsburgh #8 Run No. 11	Illinois #6 Run No. 13
1300	3.08	2.80	2.51
1325	3.13	NA	2.48
1375	3.07	2.84	2.41
1425	3.12	2.78	2.55
1475	3.07	2.78	2.50
Average	3.09 + 0.04	2.80 + 0.04	2.49 + 0.08

Atmosphere: CO/CO_2 (60/40)

TABLE 3

INTERFACIAL SURFACE TENSION OF ILLINOIS #6 COAL ASH VERSUS ANNEALING TIME, DETERMINED AT TEMPERATURE OF SESSILE DROP FORMATION

	Surface Tension, dyne/cm		
Time (min)	Run No. 13 T =1275°C	Run No. 14 T = 1250°C	Run No. 15 T = 1250°C
0-5	205	NA	238
15	244	339	255
30	278	318	259
40	249	329	278

Atmosphere: CO/CO_2

It is worth noting that the interfacial surface tension of coal ash exposed to reducing atmospheres is much less than those measured in air and $8\%H_2$-$92\%N_2$ as shown in Table 4. This is likely to be caused by the structural complexity of a melt in the surface layers of the sessile drop due to the reducing of oxygen content in a slag;

$$O_o + CO(H_2) \Longrightarrow V_o + CO_2(H_2O) \qquad [2]$$

where O_o represents an oxygen site in a silicate system, and V_o represents an oxygen deficiency. The structural reasons for the variation is not yet conclusively established. It should be noted that the interfacial surface tensions differ depending on the atmosphere in which the coals are heated.

The effect of temperature is generally noted by the increase of droplet area. In the multicomponent silicate system, nonhomogeneity is a very important factor that may change the droplet interfacial surface tension. Therefore, all experiments were perfomed on homogenized slags after measuring viscosity in a CO/CO_2 (60/40) atmosphere. Figures 1-3 show viscosity-temperature relationships along with the interfacial surface tension values. Temperature has a significant effect on the changes of the interfacial surface tension below the temperature of critical viscosity. This effect may be atributed to a nonequilibrium state due to the random distribution of surface active phases in the slag and polymerization of the silicate structure. However, there is not significant variation of η_{LV} with temperatures above T_{cr}.

Chemical composition of tested coal ashes was varied with addition of small amounts of limestone or dolomite which are used as sulfur capture agents in gasification facilities. To obtain a uniform distribution of chemical composition, coal ashes with additives underwent the same procedure described in the experimental section.

TABLE 4

INTERFACIAL SURFACE TENSION OF BEULAH, PITTSBURGH #8, AND ILLINOIS #6 MEASURED IN VARIED ATMOSPHERES, DETERMINED AT TEMPERATURE OF SESSILE DROP FORMATION

Temperature of Sessile Drop Formation (°C)	Surface Tension, dyne/cm			*Base/ Acid Ratio
	Air	H_2/N_2 (8/92)	CO/CO_2 (60/40)	
Beulah				
1285	802			0.84
1275		615		
1200			408 + 18	
Pittsburgh #8				
1275	483			0.38
1275		358		
1200			261 + 5	
Illinois #6				
1200	531			0.45
1175		334		
1275			259	

* $\frac{\text{Base}}{\text{Acid}}$ $\quad \frac{Na_2O + K_2O + CaO + MgO + Fe_2O_3}{SiO_2 + Al_2O_3 + TiO_2}$

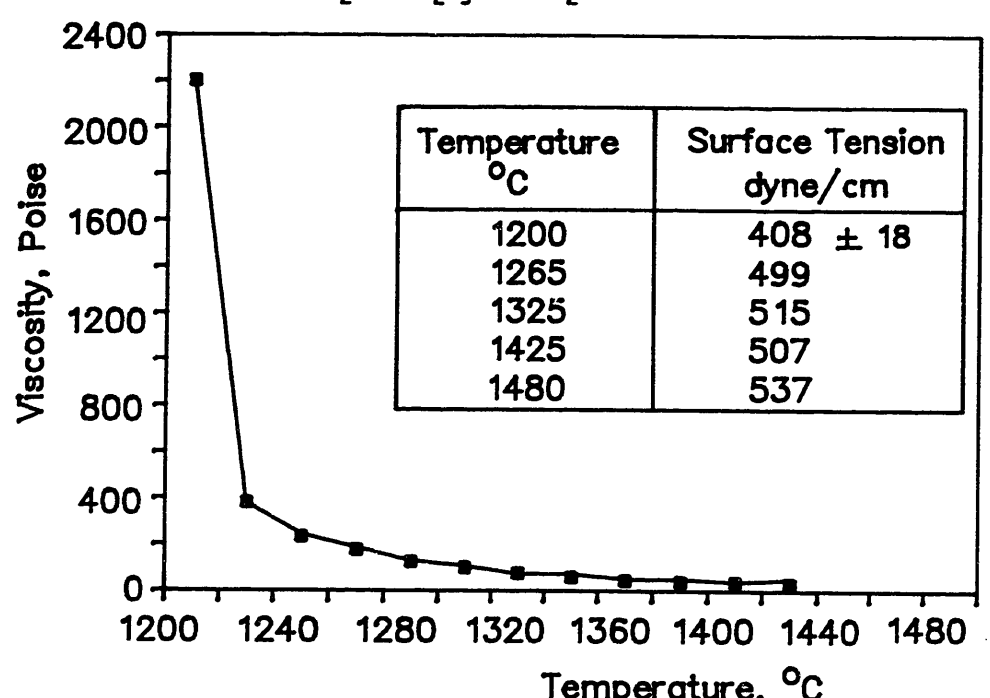

Figure 1. Viscosity-temperature relationship of Beulah slag (Run no. 7) and the values of interfacial surface tension determined for selected temperatures. Under CO/CO_2 atmosphere.

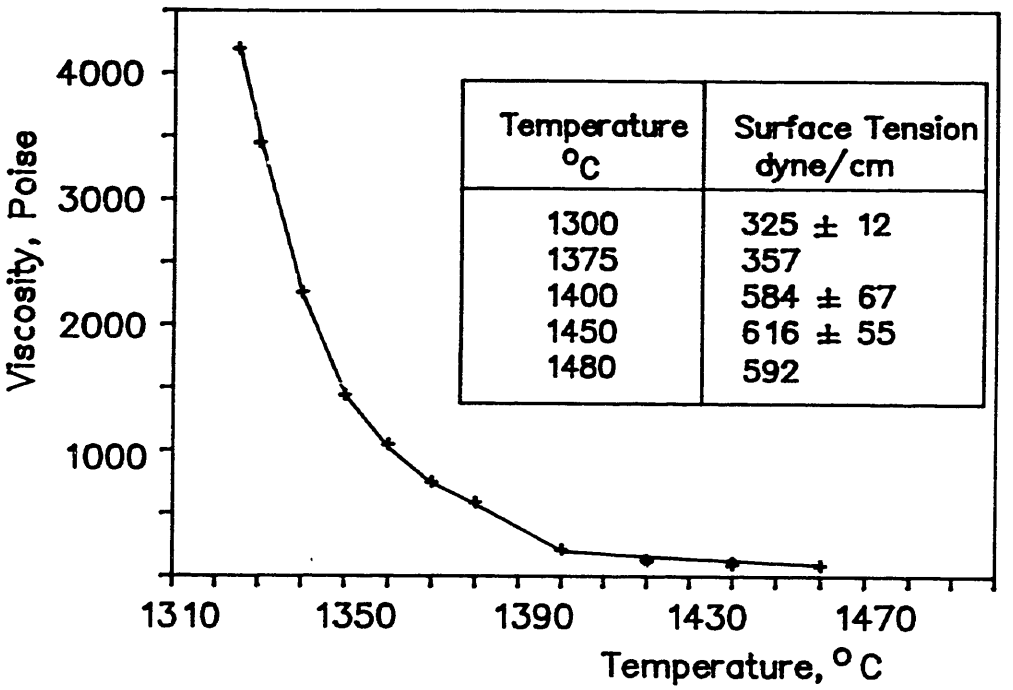

Figure 2. Viscosity-temperature relationship of Pittsburgh #8 slag (Run no. 11) and the values of interfacial surface tension determined for selected temperatures. Under CO/CO_2 atmoshere.

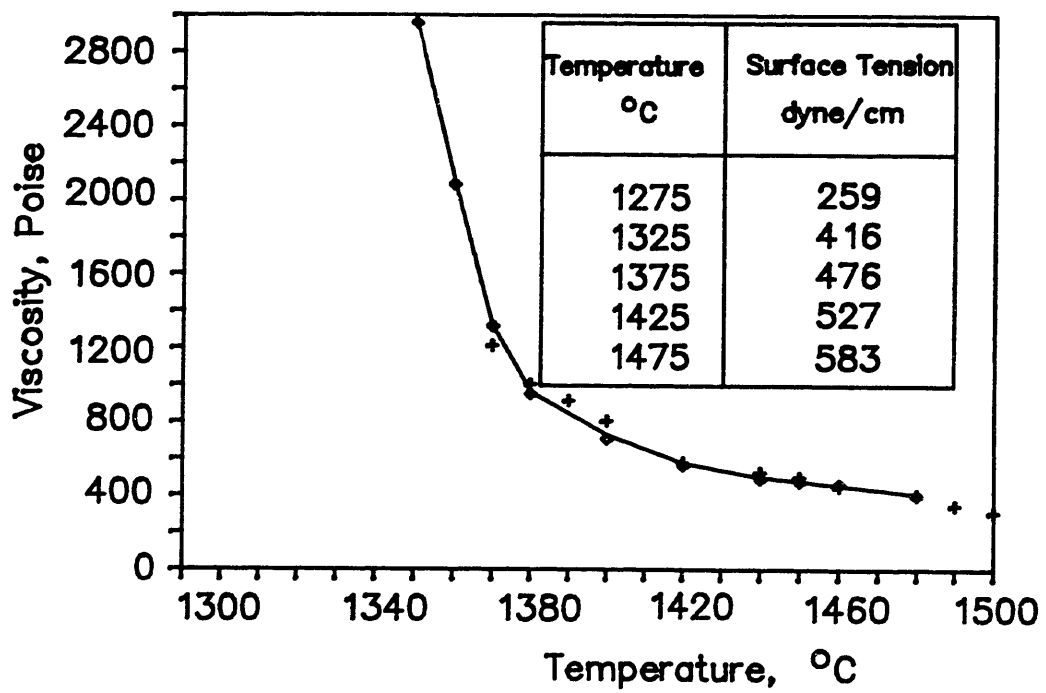

Figure 3. Viscosity-temperature relationship of Illinois #6 slag (Run no. 13) and the values of interfacial surface tension determined for selected temperatures. Under CO/CO_2 atmosphere.

Table 5 compares the values of interfacial surface tension with the base-to-acid ratio. Generally, the interfacial surface tension decreases as the base-to-acid ratio decreases. The base-to-acid ratio has been demonstrated as a useful measure of slag viscosity. Usually, viscosity decreases with the increase of the base-to-acid ratio.

TABLE 5

INTERFACIAL SURFACE TENSION OF BEULAH, PITTSBUGH #8, AND ILLINOIS #6 COAL ASHES WITH ADDITIVES, DETERMINED AT TEMPERATURE OF SESSILE DROP FORMATION

Temperature	Interfacial Surface Tension, dyne/cm			
(°C)	Coal Ash	Coal Ash + Limestone	Coal Ash + Dolomite	*Base/ Acid Ratio
	Beulah			
1200	408 + 18			0.79
1300		267 + 4		0.72
1275			419	0.90
	Pittsburgh #8			
1200	261 + 5			0.34
1250		329 + 20		0.50
1300			389 + 34	0.44
	Illinois #6			
1275	259			0.41
1250		328 + 10		0.60
1250			269 + 20	0.52

Atmosphere: CO/CO_2 (60/40)

* $\frac{\text{Base}}{\text{Acid}} = \frac{Na_2O + K_2O + CaO + MgO + FeO}{SiO_2 + Al_2O_3 + TiO_2}$

4.0 REFERENCES

1. Sangiorgi, R.; Caracciolo, G; Passerone, A. J. Mater. Sci. **1982**, 17, 2895.

2. Maze, C.; Burnet, G. Surface Sci. **1971**, 27, 411.

3. Raask, E. Trans. ASME J. Eng. Power Ser. A, **1966**, 88, 40, (ASME Paper No. 65-WA/FU-1).

4. Davies, M.W.; Hazeldean, G.S.F.; Smith P.N. Physical Chemistry of Process Metallurgy:the Richaerdon Conference; J.H.E. Feffers and R.J. Tait, Eds., Inst. Mining and Metall., London, 1973, p. 95.

3.6 Coal Science

COAL SCIENCE
EARTH RESOURCE EVALUATION AND MANAGEMENT

Quarterly Technical Progress Report
for the Period January-March 1990

by

Joseph H. Hartman, Project Manager
University of North Dakota
Energy and Environmental Research Center
Box 8213, University Station
Grand Forks, North Dakota 58202

Contracting Officer's Technical Representative: Leroy Dockter

for
United States Department of Energy
Laramie Project Office
P.O. Box 1189
2020 Grand Avenue
Suite 450
Laramie, WY 82070

May 1990

Under Cooperative Agreement No. DE-FC21-86MC10637

TABLE OF CONTENTS

COAL SCIENCE
EARTH RESOURCE EVALUATION AND MANAGEMENT

1.0 Goals and Objectives

The general "Coal Science" objectives and goals are based on the desire of the North Dakota Mining and Mineral Research Institute (MMRRI) to 1) more fully utilize coal and related geologic data currently available for integration and analysis, and 2) base interpretation of these data on well controlled test cases or examples. The focus of the first phase of the project is to setup the computerized basis for reevaluating, or evaluating for the first time, North Dakota's lignite resource in its stratigraphic and paleontologic context.

2.0 Accomplishments

During this reporting period, each component of the first year objectives were augmented including 1) acquisition, ordering, and review of computer-related hardware and software, 2) review and acquisition of field and laboratory equipment, 3) data base design evaluation, 4) computerization of a variety of coal and related geologic data, 5) geologic and paleontologic preparation of test area and related samples, 6) review and submission of applications for permission to drill in test areas on U.S. Forest Service property, and 7) preparation of papers and talks that utilized data base designs so-far implemented (see Appendix 1). These accomplishments included completion of Milestones E.1, E.2, and F.1. Milestones E.1 and E.2 represent the assessment and characterization of the stratigraphic and paleontologic data base designs and procedures for Year 1. Milestone F.1 includes the augmentation of the data base for Bowman and Slope Counties in southwestern North Dakota.

2.1 Computer Hardware and Software

Hardware. A video-capture system is now operational and will become an important part of the analysis of the stratigraphic and paleontologic context of coal. This system runs on the main data management computer (Gateway 2000-386), utilizing a PCVISIONplus framegrabber from Imaging Technology. This video system consists of a high-resolution SONY Trinitron monitor, Cohu CCD camera and lens, and a SONY thermal printer. The system uses specialized programming, such as Jandel's JAVA program, to "capture" black and white images for digitizing and numerical analysis. Initial hardware system incompatibility problems consisted of memory conflicts between video cards, capture programming, and the EVEREX cassette tape backup system. These problems were resolved by establishing protocol to reconfigure the hardware for different applications. Thus the video system runs under its own configuration to resolve its hardware specific requirements. The video system will capture images for analysis at three scales or levels of magnification: 1) macro (large objects from 10 to 500 mm in length) 2) micro (small three-dimensional objects from 1 to 50 mm in length), and 3) micro (effectively two-dimensional objects less than 1 mm in size). With the Cohu lens (12.5-73 mm

zoom) and TOYO diopters, the video system can capture a wide range of macroscale images. Experimental work continues to determine the best configuration to maximize depth of the field for close-up work of large three-dimensional objects. Relatively small specimens, or close-up study of large specimens, require macrophotography. The Cohu camera can be fitted for this type of application, and study is currently underway to acquire a low power dissecting-type microscope for this purpose. The third size range of objects is studied after thin-section type preparation with high-powered stereomicroscopes. A Zeiss microscope is available at UND-EERC for this purpose. Study is underway to adapt this microscope for video image analysis of palynomorphs from samples collected in the test areas of western North Dakota. This work represents, in part, the Ph.D. studies of Tim Kroeger, a student in the Department of Geology and Geophysics at the University of North Dakota.

Software. Video-capture and analysis programs that have been acquired for use with the hardware described above include Jandel's JAVA program and a University of California-Berkeley program known as MORPHOSYS. During the winter quarter, initial testing began to develop morphometric applications. These applications have focused mainly on paleontological specimens to determine methods for improving the accuracy and speed of taking standard measurements. In addition, video imaging provides the opportunity to effectively take "instant" photographs of objects of interest. This photographic technique saves a tremendous amount of time over conventional photography for sample documentation. Like conventional photography, but in its own peculiar way, video photography is extremely light sensitive. To facilitate the control of lighting during video photography, a standard MP3-type copy stand was rewired so that each of the four high-intensity lamps could be individually regulated. Although use of the video-capture system has just begun, it offers great promise in the numerical analysis of a variety of samples and in the incorporation of video images into other programs for display or additional analysis.

Data base design and management is founded on Symantec's program "Q&A." As has been noted previously, this program is essentially unique in its application power versus ease of use and cost effectiveness. The program is intended to be utilized for complex retrieval in various routines that provide immediate flexibility for data acquisition and reporting. Q&A is capable of using multiple external files in data management and reporting that permits data base design to employ relational-type data processing. Compared to major market data base systems, such as dBASE, rBASE, and PARADOX, Q&A provides the on-line users with the opportunity to control their data environment without elaborate ritual or protocol. In addition, Q&A provides a word-processing environment that can be employed to utilize information from constructed data bases within its "file" environment. Thus text and data can be merged in any number of formats without redesigning files. Enhancement features (e.g., bold, italics, font selection), available to word-processors, can be added to "data" to clarify and augment data presentation. During the winter quarter, additional time was spent to improve the output design of data to Hewlett-Packard laserjets. Bitstream fontware was acquired to permit the construction of PRESTIGE fonts of any size and style (e.g., bold, italic, etc.). Data base programming and desktop laserjet systems are currently undergoing major

changes in their ability to display data and images easily. "Traditional" (a few years old) techniques for displaying laserjet output will be outdated as programs (e.g., Borland's spreadsheet program QUATRO PRO) will automatically download desired fonts, and/or the laserjet itself (e.g., HP Laserjet III) will provide a wider variety of font choices. This discussion is presented to stress that data management is inextricably bound to its adequate display for analysis, interpretation, and reporting.

During the winter quarter, programming was acquired for basic data analysis, including Borland's spreadsheet QUATRO PRO and Applied Biostatistics' NTSYS-pc, which is a numerical taxonomy and multivariate analysis system of programs. QUATRO PRO is a LOTUS 123-type spreadsheet for numerical data management and display. QUATRO PRO was acquired, in part, because it provides greater data reporting control and better graphics. NTSYS-pc was acquired for numerical analysis of paleontologic data and will be used in conjunction with data obtained through video imaging.

During the fall quarter, the geologic program STRATIFACT by GRG was acquired (through other funding) for the display and analysis of geologic section data and their correlation. This version of STRATIFACT had severe limitations on importing and exporting data and in other geologic-specific functions. UND-EERC-MMRRI has a standing order for the new version when it is available (the stated date of publication has long since passed). In any case, most geologic programs, like STRATIFACT, fill particular application needs. However, most are not inherently good data managers and do not provide the flexibility of data base systems such as Q&A. My approach to data management and manipulation is to utilize data systems that, if not inherently compatible, can be modified to permit the exchange of data for specific applications. Rockware's program LOGGER was acquired to facilitate the exchange of geologic section data. LOGGER is in essence a data management system of geologic section information. Files are maintained in ASCII format, and thus data can be manipulated outside of the program. This program was received at the end of the winter quarter and has received only limited study, but it is believed that data managed in Q&A will be available for use in LOGGER for graphic display of section information. In addition to LOGGER, a module was acquired from GRG to permit the up- and downloading of NCRDS section data into STRATIFACT. The use of this module awaits the arrival of the new version of STRATIFACT.

2.2 Other Equipment Considerations

During the fall and winter quarters, consideration was given to the procurement of certain pieces of field and laboratory equipment. Decisions based on immediate needs predicated the acquisition of a RAYTECH 10-inch rock slab and trim saw for the preparation of geologic cores, lithic samples, and paleontologic specimens. In addition, acquisition of a stereomicroscope was reviewed for use with the video system.

2.3 Database Design Assessment and Characterization

During the fall and winter quarters, data base design features were considered relative to potential applications. Data bases were designed and

frequently modified for use with stratigraphic and paleontologic data. I believe a general approach has been determined. The assessment and characterization were, in part, summarized in the fall quarterly report, and are included here as part of the fulfillment of specific milestones for the winter quarter.

At present, four major file-types are employed to handle geologic and paleontologic resource information. Additional files permit access to related data of a unique nature, such as map information (e.g., publication, revision, contour interval) and coding information, such as words, abbreviations, or terms that have special meaning for sort routines. The four main file-types include: 1) geologic section or observation location information (*MNOS), 2) geologic section unit descriptions (*UNIT), 3) paleontologic location and stratigraphic information (*LOC), and 4) taxon identification information (*SPP). The prefix "*" denotes a specific file name, such as WB or PRB for the Williston or Powder River Basins. Both data files with these prefixes have the same data base design and can be automatically merged into one large data base if required.

The *MNOS files contain information on the location of geologic observations, such as surface and subsurface measured sections. The *MNOS form contains six general field categories in 99 fields, including 21 code fields for specialized sort routines. *MNOS field categories include: 1) reference information, 2) numbering systems associated with record, 3) location and land owner information 4) section thickness and elevation information, 5) litho- and chronostratigraphic information, and 6) sample/specimen information. Reference information fields contain data on the source of the information (i.e., citation), including: 1) authorship, 2) source of data, 3) project chief, 4) institutional or agency affiliation of the project chief, 5) location of observation in cross section panels, and 6) type of observation (e.g., surface measured geologic section). Numbering systems associated with the record include: 1) UND-EERC-MMRRI "M-number," 2) a reference number, associated with the source of information, such as a number specifically associated with the publication of the geologic section, 3) field number, usually referring to the original number used during field work, and 4) institutional number, referring to numbering systems employed by various agencies or institutions (e.g., NDSWC 4252 = North Dakota State Water Commission number 4252), and 5) section name, if any (e.g., Tepee Buttes section). Location fields contain information ranging in scale from general political boundaries to site specific coordinate systems: 1) nation, 2) region, 3) field area, 4) state, 5) county, 6) map reference, 7) township and range location, 8) footage from section lines, 9) longitude and latitude, 10) UTM coordinates, 11) state grid coordinates, 12) property owner information, and 13) general location comment field. *MNOS files use the MAPS file as an external lookup table to import map reference information. Section thickness and elevation information is contained in fields that automatically convert metric to English measurements, error associated with elevation interpretation, and initials of interpreter of elevation. Litho- and chronostratigraphic information is contained in fields that reference: 1) the geologic age of the measured section or observation, 2) the formations represent in the section, 3) the thickness of the formations represented in the section, 4) the completeness of the formation at this location, 5) a

general listing of the named beds in the section, 6) specific reference to a particular bed, its original name (revision from field or published identification), and unit number in the section, and 7) general stratigraphic comment field. This form also contains sample and photographic information concerning the entire section, including reference numbers for: 1) fossil localities, 2) lithic samples, 3) photographs of the section.

The corresponding or companion *UNIT file has 46 fields specific to geologic section unit reference, measurement, and description. A "unit" is a stratigraphic interval, identified by the geologist, that is sufficiently distinct from lithologies above and below to represent a discrete portion of the overall geologic section. Reference fields include: 1) M-number, 2) source of information, 3) unit number, 4) unit (bed) name, 5) original bed description, 6) formational assignment of unit, 7) and sample number(s) pertaining to the unit. Measurement fields record individual unit thicknesses and permit calculations to be made to derive unit thicknesses from a variety of original information types, depending on the nature of how the section was measured. Methods of deriving unit thickness include: 1) simple inputing of original data from described measured sections (with conversions between feet and meters), 2) calculation of unit thicknesses by measuring illustrations of geologic sections for which original data no longer exists, and 3) calculation of unit thicknesses from surface geologic sections constructed by pace and compass techniques (utilizing dip control). Description fields contain information derived from the original description or illustration of the geologic section. As noted, this data base includes a large field that permits the quotation of the description of the unit as originally interpreted. The remaining fields contain information specific to different aspects of the description of the units. Standard field types include: 1) primary rock type, 2) rock-type modifiers, 3) fresh and dry colors (GSA rock color chart), 4) sedimentary structures, 5) grain size sequences, 6) weathering profile, 7) depositional environment, and 8) fossil-indicated environment. Other fields are added as needed to manage information for specific projects or to set up data (through internal lookup tables) for loading into other programs (e.g., coding for the illustration of geologic sections).

*LOC files contain records on the location of fossil localities and is specifically designed for micro- and macro-fossil specimens. The *LOC file is similar to *MNOS files in general design, containing the nearly the same fields for reference and location data. Like the *MNOS form design, *LOC files contain a number of coding fields used for sort routines of age-related information and uses the file MAPS for map reference information. Specialized locality fields include information on: 1) litho- and chronostratigraphy, 2) collecting history, and 3) the fauna. Stratigraphic fields contain information concerning: 1) the formation and member to which the locality can be assigned, 2) the original formation used by the discoverer of the locality, 3) the elevation of the locality, 4) the footage determination of the horizon of the locality within the formation (e.g., from top or bottom), 5) the level or interval of the locality relative to other formational contacts and marker beds, 6) the measured section and unit numbers (*MNOS, *UNIT) to which the locality belongs, 7) the age of the locality, and 8) an extended comment field for additional stratigraphic considerations. Information concerning the

collecting history of the locality includes: 1) the discoverer(s) and date of discovery, 2) collector(s) and date of collecting, 3) field party chief and institutional or agency affiliation, and 4) the repository for the collections. Faunal information about the locality includes: 1) fossil groups represented at the locality (e.g., mammals, microfossils, mollusks, etc.), 2) a faunal list of identified taxa, 2) name of the individual identifying the fossils, and 3) faunal comment field concerning the preservation of the fossils.

The companion *SPP file records information on the identification of taxa at a particular locality. Field types include: 1) taxon identification, 2) a simplified classification of the taxon, 3) repository and specimen numbers, and 4) number of specimens and identification comments. Both old and revised identifications are recorded to provide a history of study on specific specimens and taxon names. The file *SPP uses the *LOC file and MCLASS files as external lookup files. Using *LOC files, the stratigraphic range of a taxon can be determined through a merge of the components of the two files. Using the MCLASS file, a simplified classification of a taxon can be automatically imported into *SPP to provide a means to summarize stratigraphic data on higher taxonomic categories.

2.4 Data Input

Substantial amounts of data have been entered in all of the four main file types (i.e., *MNOS, *UNIT, *LOC, and *SPP). External lookup files have also been constructed that maintain information on map reference data (MAPS) and fossil-classification (MCLASS). Other files record information on related information and include the following files: 1) overall locality register (LOCREG), 2) type-specimen data (TCKZOIC), 3) specimen numbers and institutional repositories (SPEC-NO), 4) taxon coding (TAXON-NO), and 5) reference bibliography (BIB). Measured section and other geological observations (*MNOS and *UNIT files) have been and continue to be entered for western North Dakota and adjacent Montana, focusing on the Slope County test area, but also in Bowman County and in the area of Fort Union in the vicinity of the Nesson Anticline in Williams and McKenzie Counties. Locality (*LOC and *SPP files) information has also been inputed for these areas and continues to be augmented. Locality information has also been inputed for the Powder River Basin for the purposes of determining the age relations between the coal-bearing strata of this basin with that of the Williston Basin. MAP data has been entered for North Dakota, Montana, Wyoming, and portions of southernmost Saskatchewan. Additional MAP file management is underway. USGS map data is being downloaded from magnetic tapes into Q&A files for greater ease of use.

2.5 Sample Preparation

Geologic and paleontologic samples of importance to interpreting the geologic context of coal-bearing strata in western North Dakota were and continue to be prepared for study. Sample analysis will include traditional and recently available techniques (video-capture) to provide stratigraphic, environmental, and biochronologic information.

2.6 Drilling-related Activity

Two sites have been proposed for drilling and geophysical logging. These sites are in northwestern Slope County and southwestern Golden Valley County, North Dakota. Data derived from drilling at these sites will add significantly to our ability to correlate and interpret the coal-bearing strata of the lower and middle Paleocene of easternmost Montana and western North Dakota. Both sites are on federal Forest Service property and require permits for access and drilling. Appropriate permit forms have been completed and will be submitted in April. An "invitation for bids" has also been drafted. This document includes the specifications and requirements for the drilling process. The bid invitation is modeled after documents used for this purpose by the North Dakota State Water Commission.

2.7 Papers & Presentations

During the winter quarter, papers and talks were prepared that utilized data inputed into the data base structure described above (see Appendix 1 for titles). The flexibility of data retrieval and reporting permitted data to be organized for convenient interpretation and construction of illustrations. Additional contributions are planned for talks and papers due during spring quarter that will serve as additional tests for the adequacy of current data base designs.

3.0 Summary and Conclusions

Substantial progress continues to be made toward establishing MMRRI geologic and paleontologic data base designs in regards to coal and its geologic context. The milestone "E. Data base assessment and characterization" has been completed for stratigraphy (E.1) and paleontology (E.2). In addition, "Data base augmentation (F.1)" for the Slope/Bowman County test area has been completed. Drill hole data for this area, however, continues to be inputed for research on coal stratigraphy and correlation. The data bases described above permit the computerization of large amounts of quantitative and descriptive geologic data and yet are relatively easy to use. Besides myself, data has been inputed by undergraduate and graduate students and support staff. Although some training is required, inputing of data that does not require interpretation is relatively straightforward. Individuals with a geologic background can input data requiring some interpretation (e.g., stratigraphic and descriptive information) using customized help information available with all fields in all files. As previously noted, the goal is to make computerized coal resource data available to the researcher as part of the analysis phase of their work. This permits a far wider range of choices in manipulating and displaying available data. The next step is to make the data available through a computer network system that allows all researchers to utilize the same data bases conveniently.

4.0 Appendix 1: Papers and Abstracts Prepared and Submitted during the Winter Quarter

Kihm, A.J., and HARTMAN, J.H., 1990, Chronostratigraphic implications of the mammal and nonmarine mollusk record of the Paleocene Fort Union Group in North Dakota: North Dakota Academy of Science, v. 44, p. 70. [accepted; to be presented and published in April].

HARTMAN, J.H., and Kihm, A.J., 1990, Chronostratigraphy of Paleocene strata in the Williston Basin, in Finkelman, R.B., Daly, D.J., Tewalt, S.J., eds., Geology and utilization of Fort Union Region lignites [submitted and accepted; to be published in Fall, 1990].

HARTMAN, J.H., 1990, Paleocene and lower Eocene nonmarine molluscan biostratigraphy of the Powder River Basin, Wyoming-Montana: Geological Society of America, Rocky Mountain Section [submitted and accepted; to be presented and published in May].